Improving existing protected areas could double their modelled threat-reduction impact

Claire Vincent[*], Elías Cisneros[†], Carlo Rondinini[‡]

June 2026

Biodiversity is essential for ecosystem stability and human well-being, but human activities have intensified pressures on nature, leading to biodiversity loss and ecosystem degradation[1]. Protected areas are considered an effective instrument for safeguarding biodiversity and are among the most widely used conservation strategies worldwide, yet assessing their ability to reduce human pressures remains difficult as it requires disentangling the effects of protection from confounding factors such as location and accessibility[2]. Here we estimate average treatment effects on terrestrial protected areas for fourteen spatial threat indicators and an overall composite index using a quasi-experimental approach. We find that the composite index is 31.5% lower for protected pixels than in matched controls, with statistically significant reductions in built area, cropland, mining, roads, powerlines, and forest loss. Threat reductions are strongest in tropical forests, where protected areas reduce threats at nearly twice the global average. Assuming that not all protected areas can eliminate all threats, we use the best-performing protected areas within comparable pressure contexts as a benchmark and estimate that existing protected areas achieve 49.2% of their model-implied, area-weighted threat-reduction potential. Furthermore, our results show that many threatened vertebrate ranges remain exposed to ongoing pressure even inside protected areas. Our analysis shows considerable room for improvement in the management of existing protected areas, and provides a decision-support framework that balances protection expansion with improvements in effectiveness to achieve the Convention on Biological Diversity's protected area target[3].

[*]Sapienza University of Rome, Global Mammal Assessment Program, Department of Biology and Biotechnologies, Viale dell'Università 32, Rome, 00185, Italy, clairelouise.vincent@uniroma1.it

[†]The University of Texas at Dallas, School of Economic, Political and Policy Sciences, 800 West Campbell Rd, Richardson, TX 75080, United States

[‡]Sapienza University of Rome, Global Mammal Assessment Program, Department of Biology and Biotechnologies, Viale dell'Università 32, Rome, 00185, Italy

1 Main text

The diversity of life on Earth is essential to the integrity, stability, and resilience of ecosystems supporting a wide range of ecosystem services, including pollination, climate regulation, nutrient cycling, and food security[1]. However, human population growth and economic development have increased pressure on biodiversity, contributing to high rates of species extinction and ecosystem degradation globally[4,5]. The main threats that contribute to the decline of biodiversity, including habitat loss, overexploitation, climate change, and invasive species, are classified by the International Union for Conservation of Nature (IUCN) using a standardized classification scheme[6,7]. This framework allows for a nuanced understanding of the ongoing and potential future drivers of biodiversity decline, as well as the role of conservation efforts in mitigating these pressures[6].

Protected areas (PAs) are among the most widespread interventions for in situ biodiversity conservation, with the aim of improving the state of biodiversity within their boundaries[8,9]. The importance of PAs has prompted the adoption of increasingly ambitious international targets for PA coverage. Target 3 of the Kunming–Montreal Global Biodiversity Framework (GBF), commonly referred to as '30×30', calls for at least 30% of land and sea to be conserved through effectively managed, equitably governed, ecologically representative, well-connected PAs and other effective area-based conservation measures by 2030, especially in areas important for biodiversity[3]. Area coverage alone is therefore not the only goal, yet worries remain about some governments claiming progress by focusing only on coverage without demonstrating meaningful protection[10]. If added protection does not reduce the pressures that cause species loss in the places where species need protection, focusing on the coverage alone will overstate progress. Together with climate change, biodiversity loss is expected to have the greatest impact on human lives in the next century[5], therefore, it is crucial that we understand the effects of our most commonly employed conservation tool.

Measuring the effectiveness of PAs at a global scale has been limited by differing conservation objectives across sites[11], heterogeneous impacts of threats affecting species[12], and the resolution and availability of data needed to assess impact[13]. Recent synthesis likewise shows that PA threat reduction is mixed, threat-specific, and highly context-dependent[14]. Yet, without global evidence on whether PAs reduce the threats driving biodiversity loss, the expected biodiversity gains from 30×30 remain difficult to quantify. Understanding whether PAs truly contribute to biodiversity conservation requires estimating counterfactual outcomes to treated sites that control for confounding factors at baseline, like habitat quality and accessibility[15,16]. Moreover, the assumption that PA coverage directly leads to improved biodiversity outcomes has been contradicted by growing evidence[17,18,19]. Existing global impact studies have provided evidence on forest loss, climate change, land-use change, and biodiversity responses in narrower settings[20,21,22,23]. Yet three questions remain unresolved at the global scale, which we address here (1) whether terrestrial PAs have a uniform effect across unassessed threats; (2) how much scope there is for further threat reduction in existing PAs; and (3) to what extent the reductions occur within the ranges of threatened species.

To assess the effect of PAs on threat abatement, we compile a global dataset of 1-km^2 terrestrial pixels with 14 spatial threat indicators. To summarize, we build a composite threat index that aggregates these fourteen individual threat indicators via a hierarchical weighting scheme that mirrors the IUCN threat classification and accounts for cross-country differences in threat prevalence (Supplementary Fig. C.2). We then compare pixels inside PAs designated during 2001–2020 with similar unprotected pixels using 1:1 Mahalanobis matching with replacement on eight pre-designation geophysical and accessibility covariates. Matching is conducted within country–biome–big-region strata, where the big-region field subdivides large countries administratively and predefined within-country control-pooling rules address sparse strata (see Methods). From this matched dataset, we calculate the Average Treatment effect on the Treated (ATT), which is the pressure contrast between PAs and similar control sites, where negative values indicate lower pressure inside PAs. This design mitigates bias from PA placement to remote areas with lower-opportunity landscapes[24]. Nonetheless, some unobserved sources of bias may remain[25,15], such as governance, enforcement capacity, or pre-existing threat trajectories.

To assess how robust our results are to these unobserved sources of bias, we test how strong any unmeasured confounding factors would need to be to invalidate our results. Additionally, to explore the sensitivity of our results to different parameter choices at each step, we conduct additional analyses. We vary the matching procedure using random sub-sampling and alternative matching procedures, and run multiple models with sequential fixed effects and additional controls. Our main results are supported by these tests (see Supplementary Information). Nonetheless, our approach focuses on a comprehensive global estimate, and caution is warranted when interpreting global-level results at the local scale.

1.1 PAs reduce threats globally

The threat level across all 14 indicators for PAs is about 53% lower than the global average. This highlights the remote location of PAs and emphasizes the need to account for observable confounders to avoid overestimation[26] (Supplementary Fig. C.1). Accounting for these systematic differences, nine of the fourteen individual threat indicators are lower within PAs at $p < 0.10$, and six are lower at $p < 0.05$: built area, cropland, mining operations, road presence, power lines, and forest loss (Fig. 1, Extended Data Table B.2). Overall, PAs reduce the composite threat indicator by 31.5% relative to matched controls.

Our results support previous studies that focused on the role of PAs in reducing built area[22] and deforestation[27,28] as we find that PAs have 41% less built area (ATT = -422 m^2, std. err. = 162, P = 0.01) and 63% less forest loss than controls (ATT = -0.06 m^2, std. err. = 0.02, P < 0.01). The conversion of natural habitat to cropland has previously been estimated to account for 18% of all human impacts within PAs[29]. Notwithstanding, we find that PAs still have 43% less cropland compared to matched controls (ATT = -1.3 %pts., std. err. = 0.3, P < 0.01). This observed beneficial effect of protection does not extend uniformly across all pressures.

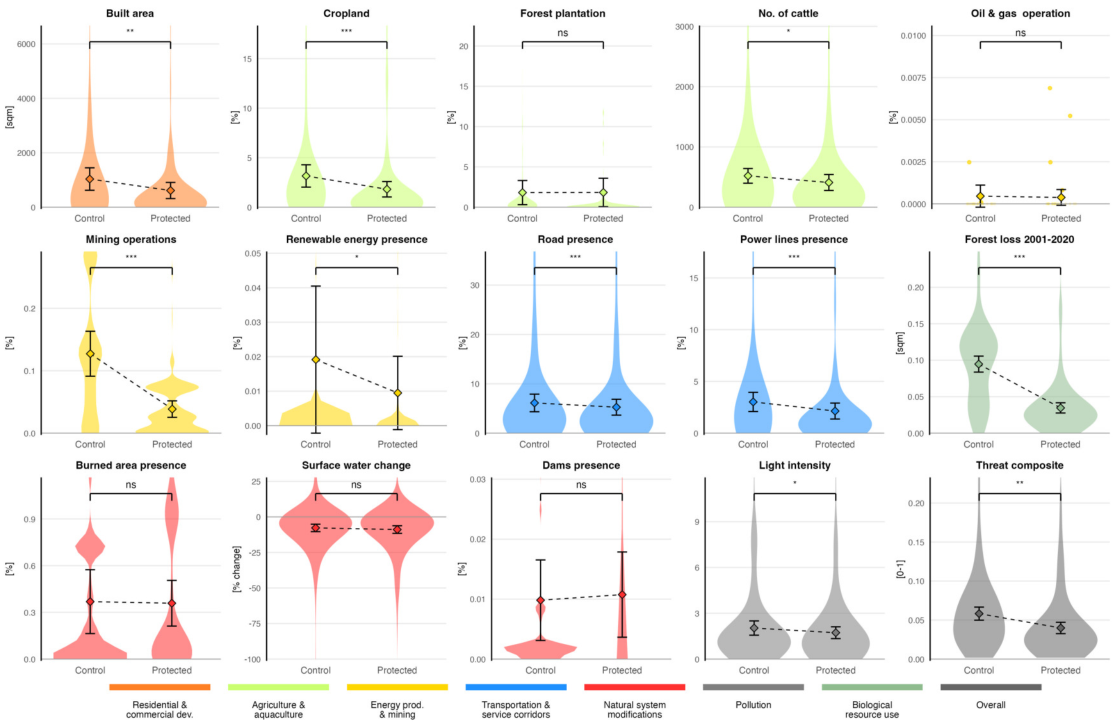

Figure 1: **Protected area effects on threat indicators.** Each panel shows the distribution of country-level mean threat values for matched control pixels (left) and protected pixels (right), separately for each of the 14 individual threat outcomes and the composite threat index. Threat levels are shown in original units (see y-axis labels). For a detailed description of threat categories and datasets, see Table B.1. The panels are coloured based on their IUCN threat categories (legend below the panels). Diamonds mark the country-weighted mean, and black whiskers show the 95% confidence intervals. The dashed line connects the two group means. The significance reflects the average treatment effect on the treated (ATT), where */ **/ *** denote p $< 0.1/0.05/0.01$, respectively, and "ns" indicates non-significant, with full regression results provided in Extended Data Table B.2.

We find no effect of land protection at a global scale for the amount of burned area (ATT = -0.01 %pts., std. err. = 0.06, P = 0.87). When fighting wildfires, priority is given to protecting people and property over wild areas, which may contribute to higher burned-area levels within PAs[30]. Furthermore, fire can be part of PA stewardship, for example, in Canada, the ecological use of fire has been widely integrated into PA management planning to meet conservation objectives[31].

Changes in water availability within PAs depend heavily on management outside their boundaries, particularly when water extraction for agriculture, industry, and human consumption happens upstream[32]. PAs play a key role in supplying freshwater, with 80% of the human population receiving their water from upstream PAs under high water stress[33]. Positive spillovers from upstream PAs can enhance freshwater availability and quality in adjacent and downstream landscapes[34], which may explain why we find no significant difference in surface water changes between PAs and controls (ATT = -1.2 %pts., std. err. = 1.3, P = 0.39). While dams disrupt original landscapes, they do secure human water resources and may establish new habitats that can favour wildlife such as waterbirds[35]. Dam sites are therefore prone to PA designation despite their known impact on wildlife[36]. With this potential bias at hand, our global estimate shows no difference for the deterrence of dams in PAs (ATT = 0.001%pts., std. err. = 0.003, P = 0.77).

In addition, PAs do not significantly reduce light intensity at the 5% level (ATT = -0.3 DN, std. err. = 0.2, P = 0.09), likely because brightly lit areas are relatively rare globally, and radiance levels are generally low outside of large cities[37]. Similarly, no significant effect of protection is found for plantation forests (ATT = 0.02 %pts., std. err. = 0.25, P = 0.95), where potential mis-management of individual sites, or power held by this industry could enable expansion into ecologically sensitive areas[38].

1.2 Threat reduction is highly variable

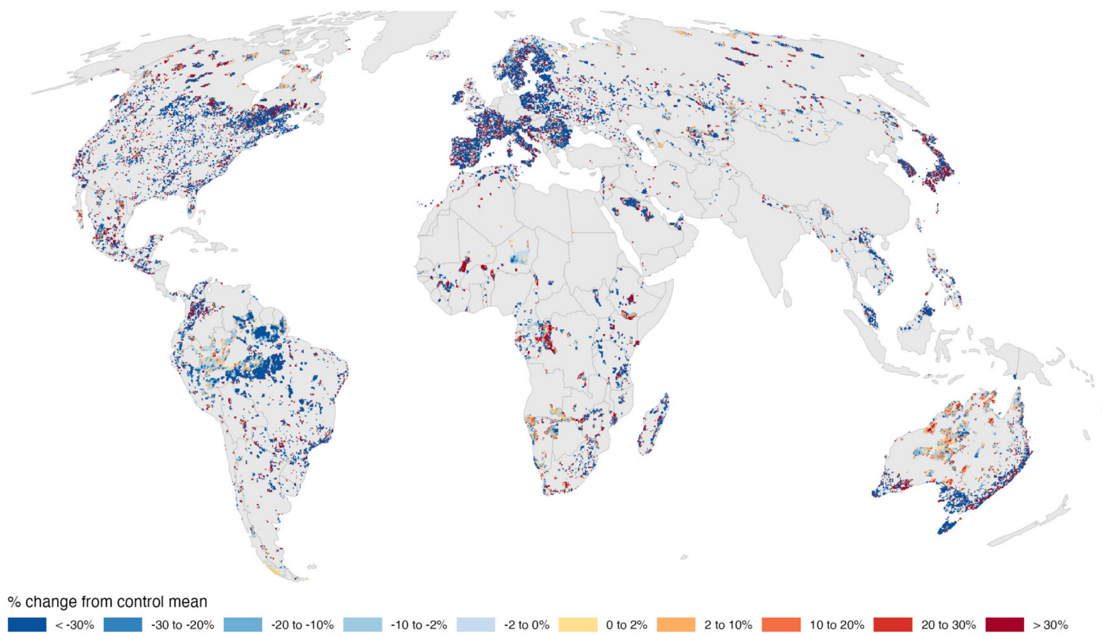

Figure 2: **Global variation in protected area pressure differences.** The percentage difference of the threat composite in assessed PAs relative to the matched control mean, aggregated to a 25 km grid. Blues indicate lower threats inside PAs, and yellow to red indicates higher threats. This is a descriptive aggregation of pixel-level matched differences and does not show local statistical uncertainty.

The global composite estimate masks substantial spatial variation in the treatment effect. Pixel-level comparisons show regional clusters of large threat reductions, including in the Amazon rainforest. They also show clusters where protected pixels have similar or higher composite threats than their matched controls, including in the Congo Basin (Fig. 2). This geographic variation may reflect differences in the underlying pressure context of individual PAs. When comparing PA-level treatment effects by matched control threat level, we find that PA effects increase substantially with baseline pressure (Extended Data Fig. B.4).

We aggregate the pixel-level effects by biome to show ecological patterns and find that half of all biomes have significantly lower threat-composite scores inside PAs (Extended Data Fig. B.1).

Because biomes group landscapes with similar climate, vegetation, and associated animal communities[39], these estimates show where PAs are most effective across broad ecological contexts. The largest reduction occurs in tropical and subtropical moist broadleaf forests, where PAs have 58% lower composite threats than matched controls (n = 3,530,516, p < 0.01). Five individual threat indicators are lower at $p < 0.05$, and eight are lower at $p < 0.10$. This includes deforestation, which is 74% lower inside PAs (n = 3,394,310, p < 0.01), the strongest biome-level deforestation reduction (Extended Data Table C.6). This biome also has the largest share of global PA area (Supplementary Table C.5). This is important because recent work reports that deforestation pressure in African portions of this biome has shifted these forests from a carbon sink to a carbon source[40].

Because conservation priorities are often defined by biodiversity hotspots rather than by biomes[41], we repeat the estimation for the 31 hotspots represented in the matched sample (Extended Data Fig. B.2). Protected areas have lower composite threats in 26 of the 31 hotspots, and the reduction is significant at the 5% level in 15 hotspots (19 at $p < 0.10$), while two hotspots show significantly higher threats inside PAs. The median hotspot reduction is 10.5% of the control mean, but the spread is wide: the largest significant reductions occur in Sundaland (63%), Wallacea (51%), and the Cerrado (31%). Threat abatement inside PAs is therefore not confined to broad ecological zones, but it is also far from uniform across the areas where the most irreplaceable biodiversity is concentrated.

Among the 107 countries retained after the covariate-balance filter, 106 yield composite estimates. PAs have negative point estimates in 90 countries and positive point estimates in 16. At the 5% level, 84 countries have significant reductions, 10 have significant increases, and 12 are not significantly different from zero (Supplementary Table C.7). Having positive point estimates does not necessarily mean countries are performing poorly overall. For example, Kenya's PAs significantly reduce five threat indices but show a 52% higher level of cattle which pushes the estimate on the threat composite to be positive. This is likely due to 70% of the protected wildlife reserves and parks in Kenya falling within rangelands[42], where traditional pastoralist management practices are part of PAs stewardship. We therefore acknowledge that all of these pressures need to be assessed within their local contexts, where their presence may not necessarily conflict with the management goals of an individual PA.

Differences in threat abatement occur within the PA network itself with variation across management category and size. Strictly managed PAs, which prioritise biodiversity conservation with limited human use, and multi-use PAs reduce overall threat levels similarly (Supplementary Table C.8), although strictly managed PAs have greater reductions for plantation forests, light pollution, roads, and deforestation (Extended Data Fig. B.3). Smaller PAs are associated with greater absolute threat reductions, yet larger PAs show stronger reductions relative to underlying threat levels of their matched controls. Large PAs are often viewed as essential for conserving vulnerable biodiversity and as more cost-effective than smaller reserves[43]. Our estimates are consistent with this view, suggesting that large PAs have greater capacity to buffer against high external pressure. The broader lesson, however, is that size and formal designation are incomplete proxies for effectiveness. Multi-use PAs reduce overall threat levels similarly to strict PAs, indicating that both management types can play an important role in threat abatement when governance and enforcement are credible[20,44]. This interpretation is consistent with evidence from FSC-certified logging concessions, where stringent forest management was associated with higher large-mammal encounter rates than conventional logging[45].

1.3 Expansion and management both offer gains

To assess whether progress toward 30×30 is constrained more by insufficient coverage or by weak threat reduction within existing PAs, we compare national PA coverage with country-level reductions (Fig. 3). Indonesia and Rwanda combine low national PA coverage (10.8% and 9.2%, respectively) with large estimated composite threat reductions (ATT = -0.051 and -0.156, or 78.9% and 36.0% below matched-control means). Indonesia passes the unchanged country-balance rule with an average absolute SMD of 0.039 and contributes 3,727 matched pairs, four PAs, and 20 treated 25-km cells to the final sample. These patterns suggest that the remaining gap in Indonesia and Rwanda lies more in coverage. By contrast, the Republic of the Congo and Zambia have substantial PA coverage (32.8% and 38.6%) but composite threat levels that are 14.4% and 8.0% higher than matched-control means, pointing instead to a management-performance gap. Interpreted alongside information on land tenure, governance, and species representation[46,47], our results can help identify national priorities that balance PA expansion with improvements in the performance of existing PAs to meet 30×30.

The coverage-performance comparison identifies where expansion or management may matter, but it does not quantify how much additional threat reduction existing PAs could plausibly deliver. We therefore use a stochastic frontier analysis (SFA) to benchmark each PA against the lowest threat levels observed among comparable PAs facing similar counterfactual pressure (Fig 4; Methods Section A.5). This frontier does not assume that PAs can eliminate all threats. Instead, it defines a model-implied best-practice benchmark conditional on pressure context. The distance between a PA's observed threat level and this frontier is the performance gap, defined here as the additional reduction that appears attainable given what similar PAs already achieve, after accounting for random noise.

Aggregating these PA-level gaps shows that the performance gap is large. We multiply each PA's observed threat reduction and estimated underperformance separately by its reported area, then sum across PAs. Across 22,090 PAs, the observed reduction is 128,320 threat-index km^2, or 49.2% of the model-implied total, while estimated underperformance is 132,732 threat-index km^2, or 50.8% (Extended Data Fig. B.5B). Closing the estimated gap would therefore approximately double the measured threat-reduction impact of the existing network. These quantities are model-implied threat-index-area units, not additional physical PA coverage.

Among the 107 countries represented in the frontier sample, the median ratio of observed to frontier-implied threat reduction is 33.0%, with substantial variation across countries (interquar-

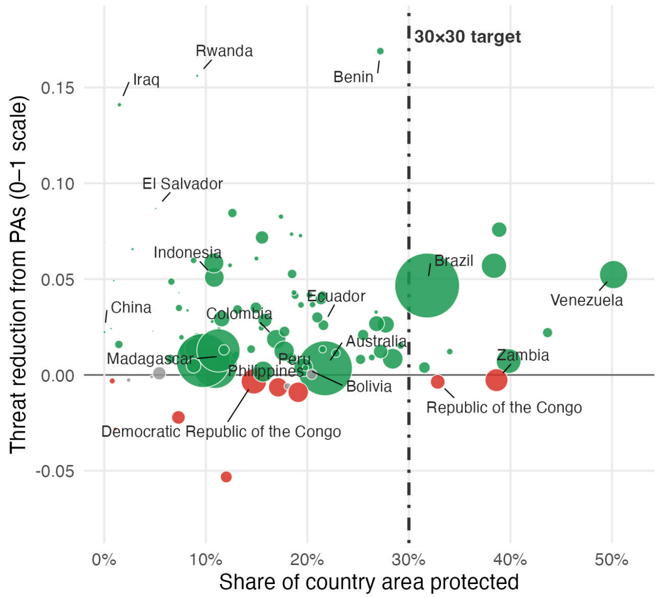

Figure 3: **PA pressure reduction and scope for expansion.** (A) The country mean of the treatment effect of PAs on the composite threat index, which has been sign-flipped so that positive values correspond to lower threats in PAs relative to matched controls. The dashed vertical line marks the 30% coverage target of the Kunming–Montreal Global Biodiversity Framework. Threats can be significantly lower in PAs (green), significantly higher in PAs (red), or insignificantly different from matched controls (gray). Bubble size is proportional to the total rasterized protected area in each country, counting PAs from all designation years rather than only the 2001–2020 assessment cohort. The fourteen most biodiverse countries are labelled as well as outliers.

tile range 15.1–63.5%; Fig. 4). Most countries fall between the no-reduction line and the frontier, indicating that PAs often reduce threats while still leaving an estimated performance gap. This variation is not captured by absolute threat levels alone. These modelled performance gaps reflect what is achievable relative to observed best practice under similar pressure conditions. They show that moving existing PAs closer to their estimated frontier could substantially increase the measured threat-reduction impact of the current network, independent of any expansion.

1.4 Pressure persists for threatened species

PAs are intended to safeguard biodiversity and their true impact depends on how well they abate pressures on biodiversity. We estimate PA coverage for 7,165 threatened terrestrial vertebrates (mammals, amphibians, reptiles, and birds classified as Vulnerable, Endangered, or Critically Endangered on the IUCN Red List). Of these, we also estimate species-level treatment effects on the composite threat index for 3,310 species, selecting complete matched pairs according to whether the protected pixel falls within each species' geographic range (Supplementary Fig. C.3). Our impact estimation again focuses on PAs designated during 2001–2020, however, for per-species coverage calculations, we use all PAs regardless of their designation year. On average, threatened species have 28.6% of their range inside any PA with substantial variation across taxa including 35.4% (median = 22.8%, n = 2,900) for amphibians, 25.4% (median = 15.9%, n = 1,355) for mam-

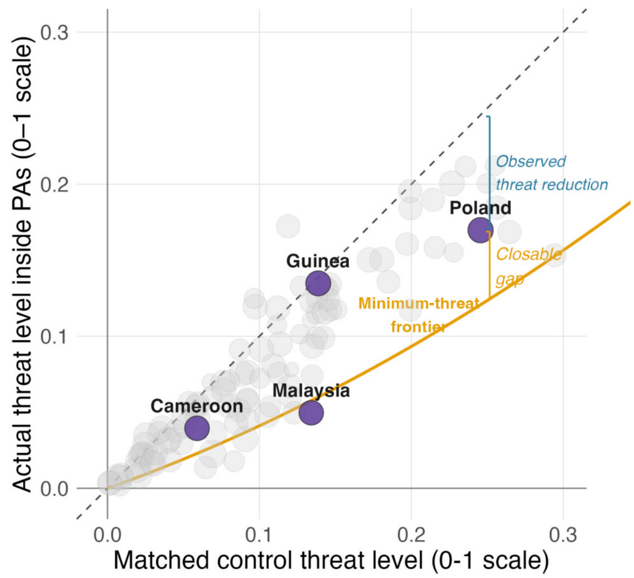

Figure 4: **Threat mitigation performance gap.** Each country is plotted by mean threat composite score inside PAs against matched controls (0–1 scale), where points below the diagonal indicate lower threats inside PAs than outside. The minimum-threat frontier (yellow line) represents the best-case threat level achievable given a country's pressure context, and the closable performance gap is the vertical distance between a country's observed PA threat level and the frontier. Bubble area is proportional to total PA area. Cameroon and Malaysia have similar threat levels inside PAs but Malaysia lies closer to the frontier, reflecting stronger reductions relative to comparable PAs globally. Poland achieves a large absolute reduction yet retains a meaningful performance gap. Guinea sits close to the diagonal, indicating little additional threat reduction beyond unprotected areas.

mals, 20.0% (median = 10.6%, n = 1,234) for birds, and 25.9% (median = 12.3%, n = 1,676) for reptiles (Supplementary Figs. C.9–C.12). Notably, there are 1,378 species (19.2%) that are not covered by any PA. These coverage gaps are consistent with previous coverage gap analyses that focused on threatened mammals[48], and amphibians[49].

Yet coverage alone does not establish that protection reduces pressure within a species' range. Among the 3,310 species with estimable range-based regressions, median threat reductions are similar across taxonomic groups: 27% for mammals, 26% for amphibians, 25% for birds, and 24% for reptiles (all bootstrap $P < 0.001$; Fig. 5). Species-level estimates nevertheless vary widely, and some species have higher pressure in protected pixels than in their matched controls. Assessing pressure reduction inside PAs is crucial for species survival because PAs are increasingly the last strongholds for many species[50,51].

At the individual species level, five illustrative range-restricted species whose mapped ranges lie completely inside PAs have significantly higher threat composite scores in protected pixels than in their matched controls. The Australian Room's skink (*Egernia roomi*, CR) and the Mexican Puebla treefrog (*Lithobates pueblae*, CR) face threat levels inside PAs that are approximately twice those of matched unprotected areas. The Chin Hills nuthatch (*Sitta victoriae*, EN), a bird endemic to a single mountain range in Myanmar, shows a 62% higher threat score inside its fully protected

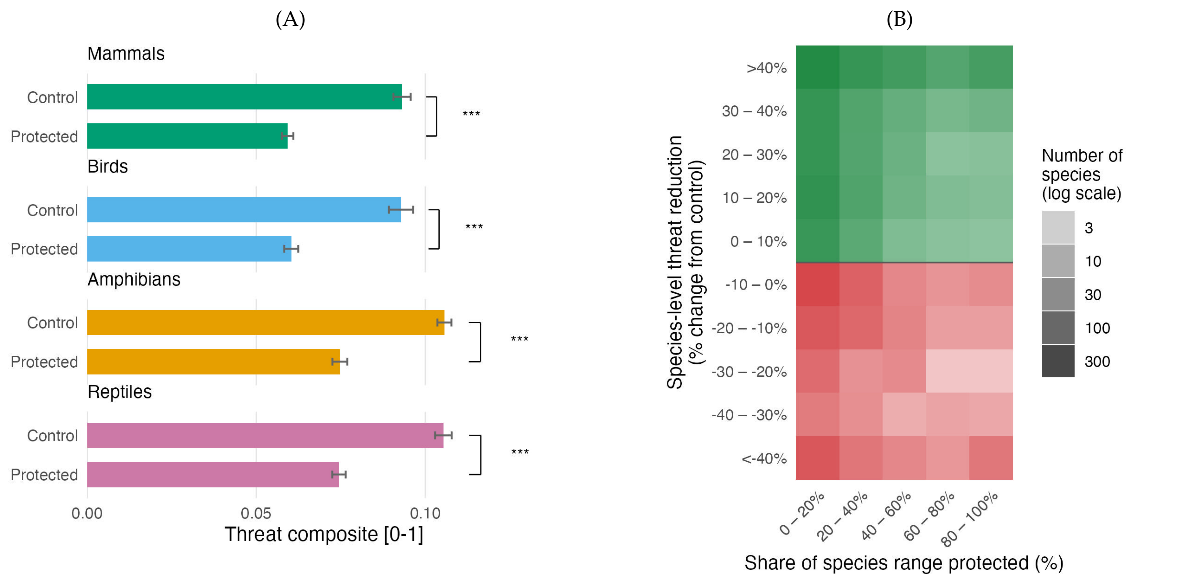

Figure 5: **Threat reduction in threatened species ranges.** (A) For each vertebrate taxon, bars show the median species-specific matched-control threat level and the median implied protected threat level, $\bar{Y}^{s,0} + \delta_s$. Whiskers show ± 1 approximate bootstrap standard error, derived from the width of the 95% percentile interval across 2,000 within-taxon species resamples. */ **/ *** denote two-sided bootstrap $p < 0.1/0.05/0.01$ for the median raw-scale species effect, respectively. See Supplementary Figs. C.9–C.12 for per-species detail. (B) Species-level threat reductions, $-\pi_s$, for threatened terrestrial vertebrates with finite range-based regression estimates ($n = 3{,}310$), plotted against the share of each species' mapped range inside a protected area. Positive values indicate lower threats inside PAs. Green indicates positive reductions, red indicates negative reductions (threat increases), and darker shading indicates more species. Cells report the number of species in each bin. The two outer reduction bins collect values below -40% and above 40%, so no finite range-based regression estimate is omitted.

range ($p < 0.01$, n = 229 pairs). Both the dwarf gecko (*Lygodactylus mirabilis*, CR) and the Lac Alaotra gentle lemur (*Hapalemur alaotrensis*, CR), one of the world's most range-restricted primates, occur in Madagascar and have threat levels 37% ($p < 0.01$, n = 26 pairs) and 27% ($p < 0.01$, n = 218 pairs) above matched controls, respectively. These cases highlight the increased vulnerability that range-restricted endemics face[48], as they depend on the performance of the few PAs where they occur. Although range-restricted species are an extreme case, similar results were found for some large-range species. For example, the Philippine Pangolin (*Manis culionensis*, CR), which has 89% of its 13,000 km^2 range protected, has 46% higher threats in its PAs ($p < 0.01$, n = 1,203 pairs).

The coverage-performance matrix is concentrated in lower-coverage bins, while estimated threat reductions span a wide range (Fig.5B). There is no clear correlation between coverage and performance: species with higher estimated threats in protected pixels occur across all coverage bins, and well-covered species span a range of threat-reduction outcomes. It is well established that PA designation without active management and enforcement delivers little measurable benefits to biodiversity[52,23]. Our results show that this gap between designation and performance is widespread across the global PA network, and that species protection is constrained by both coverage and performance.

1.5 Conclusions

Area-based targets like 30×30 are effective in practice because they are simple to communicate and monitor, but achieving only their quantitative aspects without measuring their qualitative outcomes provides limited ecological relevance[10,53]. With 30×30 unlikely to be fully achieved within the remaining timeframe, pushing for rapid PA designation risks ineffective or even harmful solutions[54]. Our results underscore the need to shift the conservation agenda from expanding the PA network to improving the threat mitigation of existing sites and quantifying the performance and species coverage gaps that remain. A fundamental gap in the current Global Biodiversity Framework is the absence of any quantitative indicator for PA effectiveness[55]. Beyond 2030, to have a meaningful impact on biodiversity, area-based targets must be complemented by measurable performance targets to ensure that effectiveness is not ignored. The framework developed here provides an empirical foundation from which such targets could be derived, offering perhaps not a uniform percentage across the globe but rather a quantitative target that accounts for the underlying pressure context of individual PAs, creating more realistic and achievable goals.

References

1. IPBES. Global assessment report on biodiversity and ecosystem services of the intergovernmental science-policy platform on biodiversity and ecosystem services. Tech. Rep., Zenodo (2019). URL https://zenodo.org/record/5657041.

2. Rodrigues, A. S. L. & Cazalis, V. The multifaceted challenge of evaluating protected area effectiveness. *Nature Communications* **11**, 5147 (2020).

3. CBD. Kunming-montreal global biodiversity framework. Tech. Rep., Secretariat of the Convention on Biological Diversity (2022).

4. Ceballos, G. *et al.* Accelerated modern human–induced species losses: Entering the sixth mass extinction. *Science Advances* **1**, e1400253 (2015).

5. Pörtner, H.-O. *et al.* Ipbes-ipcc co-sponsored workshop report on biodiversity and climate change. Tech. Rep., Zenodo (2021). URL https://zenodo.org/record/4782538.

6. Salafsky, N. *et al.* A standard lexicon for biodiversity conservation: Unified classifications of threats and actions. *Conservation Biology* **22**, 897–911 (2008).

7. Salafsky, N. *et al.* Classification of direct threats to the conservation of ecosystems and species 4.0. *Conservation Biology* **39**, e14434 (2025).

8. Langhammer, P. F. *et al.* The positive impact of conservation action. *Science* **384**, 453–458 (2024).

9. Maxwell, S. L. *et al.* Area-based conservation in the twenty-first century. *Nature* **586**, 217–227 (2020).

10. Geldmann, J. The world could reach 30% protection by 2030, and still fail to conserve biodiversity without effective and well-located protected areas. *Conservation Letters* **19**, e70030 (2026).

11. Coad, L. *et al.* Measuring impact of protected area management interventions: current and future use of the global database of protected area management effectiveness. *Philosophical Transactions of the Royal Society B: Biological Sciences* **370**, 20140281 (2015).

12. Thomson, J. *et al.* Spatial conservation action planning in heterogeneous landscapes. *Biological Conservation* **250**, 108735 (2020).

13. Ridley, F. A. *et al.* Global mismatches between threat mapping research effort and the potential of threat abatement actions to reduce extinction risk. *Conservation Biology* **38**, e14271 (2024).

14. Pulido-Chadid, K. *et al.* A systematic review of the effectiveness of protected areas at reducing threats to biodiversity. *Preprint* (2025). URL https://www.researchsquare.com/article/rs-7046705/v1.

15. Geldmann, J., Jones, J. P. G., Wauchope, H. & Ferraro, P. J. Causal claims, causal assumptions and protected area impact. *Nature* **638**, E40–E41 (2025). URL http://dx.doi.org/10.1038/s41586-024-08512-8.

16. Correia, H. E. *et al.* Best practices for moving from correlation to causation in ecological research. *Nature Communications* **17**, 1981 (2026).

17. Pressey, R. L., Visconti, P. & Ferraro, P. J. Making parks make a difference: poor alignment of policy, planning and management with protected-area impact, and ways forward. *Philosophical Transactions of the Royal Society B: Biological Sciences* **370**, 20140280 (2015). URL https://royalsocietypublishing.org/doi/10.1098/rstb.2014.0280.

18. Ribas, L. G. d. S., Pressey, R. L., Loyola, R. & Bini, L. M. A global comparative analysis of impact evaluation methods in estimating the effectiveness of protected areas. *Biological Conservation* **246**, 108595 (2020). URL https://www.sciencedirect.com/science/article/pii/S0006320719319032.

19. Baylis, K. *et al.* Mainstreaming impact evaluation in nature conservation. *Conservation Letters* **9**, 58–64 (2016).

20. Abman, R. Rule of law and avoided deforestation from protected areas. *Ecological Economics* **146**, 282–289 (2018). URL https://www.sciencedirect.com/science/article/pii/S0921800917311473.

21. Tang, Y. *et al.* Tropical forest carbon offsets deliver partial gains amid persistent over-crediting. *Science* **390**, 182–187 (2025).

22. Li, G. *et al.* Mixed effectiveness of global protected areas in resisting habitat loss. *Nature Communications* **15**, 8389 (2024). URL https://www.nature.com/articles/s41467-024-52693-9. Publisher: Nature Publishing Group.

23. Wauchope, H. S. *et al.* Protected areas have a mixed impact on waterbirds, but management helps. *Nature* **605**, 103–107 (2022).

24. Joppa, L. N. & Pfaff, A. High and far: Biases in the location of protected areas. *PLOS ONE* **4**, e8273 (2009). URL https://journals.plos.org/plosone/article?id=10.1371/journal.pone.0008273. Publisher: Public Library of Science.

25. Ferraro, P. J. & Hanauer, M. M. Advances in measuring the environmental and social impacts of environmental programs. *Annual Review of Environment and Resources* **39**, 495–517 (2014).

26. Christie, A. P. *et al.* Simple study designs in ecology produce inaccurate estimates of biodiversity responses. *Journal of Applied Ecology* **56**, 2742–2754 (2019).

27. Black, B. & Anthony, B. P. Counterfactual assessment of protected area avoided deforestation in cambodia: Trends in effectiveness, spillover effects and the influence of establishment date. *Global Ecology and Conservation* **38**, e02228 (2022).

28. Shah, P., Baylis, K., Busch, J. & Engelmann, J. What determines the effectiveness of national protected area networks? *Environmental Research Letters* **16**, 074017 (2021).

29. Vijay, V. & Armsworth, P. R. Pervasive cropland in protected areas highlight trade-offs between conservation and food security. *Proceedings of the National Academy of Sciences* **118**, e2010121118 (2021).

30. Ward, M. *et al.* Impact of 2019–2020 mega-fires on australian fauna habitat. *Nature Ecology & Evolution* **4**, 1321–1326 (2020).

31. Wang, W., Wu, W., Guo, F. & Wang, G. Fire regime and management in Canada's protected areas. *International Journal of Geoheritage and Parks* **10**, 240–251 (2022).

32. Bastin, L. *et al.* Inland surface waters in protected areas globally: Current coverage and 30-year trends. *PLOS ONE* **14**, e0210496 (2019).

33. Harrison, I. J. *et al.* Protected areas and freshwater provisioning: a global assessment of freshwater provision, threats and management strategies to support human water security. *Aquatic Conservation: Marine and Freshwater Ecosystems* **26**, 103–120 (2016).

34. Cumming, G. S. *et al.* Social-ecological contributions of protected areas to their surroundings. *One Earth* **8** (2025). URL https://www.cell.com/one-earth/abstract/S2590-3322(25)00288-X.

35. Thieme, M. L. *et al.* Dams and protected areas: Quantifying the spatial and temporal extent of global dam construction within protected areas. *Conservation Letters* **13**, e12719 (2020).

36. Wu, H. *et al.* Effects of dam construction on biodiversity: A review. *Journal of Cleaner Production* **221**, 480–489 (2019).

37. Kyba, C. C. M. *et al.* Artificially lit surface of earth at night increasing in radiance and extent. *Science Advances* **3**, e1701528 (2017). URL https://www.science.org/doi/10.1126/sciadv.1701528. Publisher: American Association for the Advancement of Science.

38. Poor, E. E., Frimpong, E., Imron, M. A. & Kelly, M. J. Protected area effectiveness in a sea of palm oil: A sumatran case study. *Biological Conservation* **234**, 123–130 (2019).

39. Olson, D. M. *et al.* Terrestrial ecoregions of the world: A new map of life on earth. *BioScience* **51**, 933 (2001). URL https://academic.oup.com/bioscience/article/51/11/933-938/227116.

40. Rodríguez-Veiga, P. *et al.* Loss of tropical moist broadleaf forest has turned africa's forests from a carbon sink into a source. *Scientific Reports* **15**, 41744 (2025).

41. Myers, N., Mittermeier, R. A., Mittermeier, C. G., da Fonseca, G. A. B. & Kent, J. Biodiversity hotspots for conservation priorities. *Nature* **403**, 853–858 (2000).

42. Ogutu, J. O. *et al.* Extreme wildlife declines and concurrent increase in livestock numbers in kenya: What are the causes? *PLOS ONE* **11**, e0163249 (2016).

43. Armsworth, P. R., Cantú-Salazar, L., Parnell, M., Davies, Z. G. & Stoneman, R. Management costs for small protected areas and economies of scale in habitat conservation. *Biological Conservation* **144**, 423–429 (2011).

44. Nelson, A. & Chomitz, K. M. Effectiveness of strict vs. multiple use protected areas in reducing tropical forest fires: A global analysis using matching methods. *PLoS ONE* **6**, e22722 (2011).

45. Zwerts, J. A. *et al.* Fsc-certified forest management benefits large mammals compared to non-fsc. *Nature* **628**, 563–568 (2024). URL http://dx.doi.org/10.1038/s41586-024-07257-8.

46. Dudley, N. & Stolton, S. Best practice in delivering the 30x30 target: Protected areas and other effective area-based conservation measures. Tech. Rep., The Nature Conservancy and Equilibrium Research (2023). A report for the UK Department for Environment, Food and Rural Affairs (DEFRA).

47. Zhang, Y. *et al.* Governance and conservation effectiveness in protected areas and indigenous and locally managed areas. *Annual Review of Environment and Resources* **48**, 559–588 (2023). URL https://www.annualreviews.org/content/journals/10.1146/annurev-environ-112321-081348. Publisher: Annual Reviews.

48. Williams, D. R., Rondinini, C. & Tilman, D. Global protected areas seem insufficient to safeguard half of the world's mammals from human-induced extinction. *PNAS* **119**, e2200118119 (2022).

49. Sze, J. S. *et al.* Indigenous peoples' lands are critical for safeguarding vertebrate diversity across the tropics. *Global Change Biology* **30**, e16981 (2024).

50. Pacifici, M., Di Marco, M. & Watson, J. E. M. Protected areas are now the last strongholds for many imperiled mammal species. *Conservation Letters* **13**, e12748 (2020).

51. Mi, C. *et al.* Global protected areas as refuges for amphibians and reptiles under climate change. *Nature Communications* **14**, 1389 (2023).

52. Coad, L. *et al.* Widespread shortfalls in protected area resourcing undermine efforts to conserve biodiversity. *Frontiers in Ecology and the Environment* **17**, 259–264 (2019).

URL https://onlinelibrary.wiley.com/doi/abs/10.1002/fee.2042. _eprint: https://onlinelibrary.wiley.com/doi/pdf/10.1002/fee.2042.

53. Carroll, C. & Noss, R. F. How percentage-protected targets can support positive biodiversity outcomes. *Conservation Biology* **36**, e13869 (2022).

54. Reed, J. *et al.* Avoid cherry-picking targets and embrace holistic conservation to pursue the global biodiversity framework. *Conservation Letters* **18**, e13104 (2025).

55. Geldmann, J. *et al.* Essential indicators for measuring site-based conservation effectiveness in the post-2020 global biodiversity framework. *Conservation Letters* **14**, e12792 (2021). URL https://onlinelibrary.wiley.com/doi/abs/10.1111/conl.12792. _eprint: https://onlinelibrary.wiley.com/doi/pdf/10.1111/conl.12792.

56. Gumbs, R. *et al.* The edge2 protocol: Advancing the prioritisation of evolutionarily distinct and globally endangered species for practical conservation action. *PLOS Biology* **21**, e3001991 (2023).

57. Isaac, N. J. B., Turvey, S. T., Collen, B., Waterman, C. & Baillie, J. E. M. Mammals on the edge: Conservation priorities based on threat and phylogeny. *PLOS ONE* **2**, e296 (2007).

A Methods

A.1 Data

PA data were taken from the February 2026 version of the World Database on Protected Areas (WDPA) and the World Database on Other Effective Area-based Conservation Measures[35]. A grid cell is considered treated if it falls within a PA designated between 2001 and 2020. PAs smaller than 1 km^2, point-only PAs, and UNESCO-MAB Biosphere Reserves are excluded[36]. Where PAs overlap, we assign the grid cell to the protected area with the earliest designation year and use that protected area's IUCN category and reported area. Control cells are those outside any PA boundary, with an additional 5 km buffer around all PAs removed to avoid spillover effects[19]. To ensure data quality and comparability, we excluded small island states and countries with insufficient or extremely low biodiversity coverage. The resulting unmatched matching input contains 127,314,386 eligible pixels across 157 countries. Matching produces 6,064,399 protected–control pairs across 145 countries before country-level balance filtering. Applying the unchanged average $|\text{SMD}| \leq 0.10$ rule yields the final analysis sample of 5,711,528 matched pairs, 107 countries, and 22,090 protected areas. Full details are provided in the Supplementary Information.

We use publicly available global pressure maps corresponding to 14 spatial threat indicators, mapped to the IUCN Red List threat classification scheme[6]. The original data sources are provided in Extended Data Table B.1 and explained in detail in the Supplementary Information. Maps at different resolutions are resampled to 1 km^2 resolution and reprojected to Mollweide equal-area projection in GRASS GIS v8.3.

We construct a continuous composite threat index that summarises the overall intensity of these threats at each pixel on a 0–1 scale. Each indicator is first normalised globally using winsorized min-max scaling. Indicators are then aggregated within each IUCN category, ensuring that each category contributes equally as a group regardless of how many individual indicators it contains. We also use country-specific prevalence weights so that threats more common in a given country contribute more to the national index. Full details of the weighting scheme are provided in the Supplementary Information.

We retrieved threatened vertebrate species ranges (mammals, reptiles, and amphibians) from the IUCN Red List version 2025-1[38] and threatened bird ranges from the Birds of the World dataset[39]. We included all species classified as Vulnerable, Endangered, or Critically Endangered with available geographic range data, yielding 7,165 species (2,900 amphibians, 1,234 birds, 1,355 mammals, 1,676 reptiles). Pixel-level biodiversity is measured as threatened-species counts from rasterized range maps.

For the heterogeneity analysis (Extended Data Fig. B.4A), we additionally used total species richness across all Red List categories[40] and several land-use pressure proxies. Full details are provided in the Supplementary Information.

A.2 Matching procedure

We compared each protected 1-km pixel with an unprotected pixel that was similar before designation and located in the same country and biome. This design reduces bias from non-random PA placement, because PAs are often established in places that differ systematically from unprotected land[8].

Based on previous studies[33,10,11] and due to the biased placement of PAs in the landscape where they tend to be in places that are at high elevations and in areas that are not important for economic activities[24], we chose the following continuous matching covariates: agricultural suitability, human population density, travel time to nearest city of 50,000 or more people, tree cover, elevation, slope, total annual precipitation, and mean annual temperature. All covariate datasets were from the year 2000 or before to ensure they represent the pre-designation state. Country is always matched exactly. Biome and big-region strata are retained when at least 20 controls are available; the big-region field subdivides Australia, Brazil, Canada, and Russia by administrative region and is zero elsewhere. For sparser strata, the donor pool expands within the same country and, in these four large countries, remains within the same biome. It should be noted that we avoided obvious confounding variables, for example soil type, soil fertility, soil quality index, and soil nutrient levels since they are all related to agricultural suitability. Each matching covariate was assessed and the reasoning for including each variable is provided in the Supplementary Information together with the original data sources.

We tested for multicollinearity between covariates using variance inflation factors (VIFs), calculated on random subsamples of 200,000 observations before and after matching. All eight continuous matching covariates had a VIF score below 5 in both samples (Supplementary Table C.1), therefore there is a low likelihood of high correlation between the variables. Additionally, collinearity among covariates is not as problematic with matching as in other methods used for impact evaluation such as parametric regression models[13]. Within each effective matching stratum, we retain every substantively varying covariate and omit a covariate only if it has fewer than two unique values or a relative standard deviation, $\mathrm{sd}(x)/\max(1,|\bar{x}|)$, of at most 10^{-6}. Every omission and diagnostic is recorded in the matching manifest, which fixes the approved omission set in advance and fails if the realised set differs. Across the 668 strata this rule omits 67 stratum–covariate combinations in 62 strata, confined to three covariates: tree cover (47), agricultural suitability (15), and human population density (5). All eight covariates are retained in every remaining stratum. We standardised the data to Mollweide equal-area projection at 1x1 km resolution in GRASS GIS v8.3.

We used one control to one treatment Mahalanobis nearest-neighbour matching with replacement, implemented with the *Matching* package in R[14]. Mahalanobis matching accounts for potential collinearity among the continuous covariates considered at each pixel[11]. The auditable matching contract contains 668 country–biome–big-region strata and records source counts, donor-pool scope, selected and omitted covariates, output hashes, and pair counts for every stratum. Matching yields 6,064,399 pairs across 145 countries before balance filtering. The final dataset retains

5,711,528 matched pairs across 107 countries and 22,090 protected areas after applying the country-balance rule (Supplementary Table C.1 & Supplementary Figure C.1). Supplementary Figure C.5 shows that the main ATT on the composite threat index is stable across alternative matching specifications (covariate set, matching ratio, with/without replacement, propensity-score matching, and coarsened exact matching) and estimation variants applied to random 1% subsamples.

A.3 Impact estimation

We estimate conditional differences associated with PA status for fourteen measured threat indicators, the any-threat indicator, and the threat composite (Extended Data Table B.1).On the matched sample, we estimate the average treatment effect on the treated (ATT) for each threat outcome by comparing protected pixels with their matched unprotected controls. This counterfactual contrast is estimated using an ordinary least squares (OLS) regression of the form:

$$Y_{icb}^{j} = \beta T_i + \gamma_c + \mu_b + \varepsilon_i \tag{1}$$

where Y_{icb}^{j} is the observed level of threat j for pixel i that is located in country c and biome b. T_i is a binary indicator equal to one if pixel i lies inside a PA and zero for its matched control. γ_c denotes country fixed effects and μ_b denotes biome fixed effects. Robustness checks vary the fixed-effect structure, add matching covariates as control variables, use PA fixed effects, and use alternative functional forms, and our estimates remain stable across these specifications (Supplementary Table C.2). ε_i is the error term. The coefficient of interest β captures the ATT where a negative estimate indicates that PAs have lower threat levels relative to matched controls, while a positive estimate indicates higher threat levels inside PAs. Combining matching with regression adjustment improves robustness to residual covariate imbalance[15]. Standard errors are clustered at the country level to account for spatial correlation of outcomes within countries. In some cases, global threat data were collected before certain PAs had been officially designated, therefore our results capture differences between protected and unprotected lands across the study period rather than a before–after comparison for every threat at every site.

For every outcome, a matched pair enters the estimation only when the protected member passes the outcome-specific target filter and the outcome is observed for both the protected pixel and its matched control; both observations are then retained or excluded together. For threats with limited geographic coverage, such as wood and pulp plantations, oil and gas extraction, mining, renewable energy, fire, and dams, the protected-side target filter restricts estimation to countries where the threat is observed, ensuring that estimates are not driven by structural zeros. We repeat the analysis by PA characteristics, classifying PAs as strictly protected (IUCN categories Ia – IV) or multi-use (IUCN categories V and VI) and categorizing PAs into four bins according to their size: less than 10 km^2, 10-500 km^2, 500-2000 km^2, and over 2000 km^2. National-level estimates are obtained from within-country regressions with heteroskedasticity-robust standard errors. For the national-level analysis, we restrict the sample to countries where matching achieved adequate covariate balance, defined as an average absolute standardized mean difference (SMD) across all covariates of 0.10 or less. Of the 145 countries represented before this filter, 107 meet the threshold and 38 are excluded to reduce residual imbalance.

Figure 1 reports observed country-level means, which are unadjusted. As a complementary summary that conditions on the same fixed effects as equation (1), we additionally compute an adjusted protected level and an adjusted counterfactual control level for every outcome. Both are standardized over the protected observations in the outcome-specific estimation sample,

$$\widehat{M}(g) = \frac{1}{N_1} \sum_{i:\, T_i=1} \widehat{Y}_i(g), \qquad g \in \{0,1\}, \tag{2}$$

where $\widehat{Y}_i(g)$ is the fitted value for observation i with the treatment indicator set to g. Under this additive model and protected-sample standardization the adjusted protected level equals the observed protected mean, the adjusted control level is the counterfactual protected-sample mean in the absence of protection, and the two levels differ by exactly the ATT, $\widehat{M}(1) - \widehat{M}(0) = \hat{\beta}$. Uncertainty for these levels comes from a country-pairs bootstrap in which each of 499 valid draws resamples countries with replacement, re-estimates the full country and biome fixed-effect model, and recomputes both levels over the protected observations represented in that draw; a draw is rejected and replaced if the predicted protected-minus-control gap does not reproduce its own refitted treatment coefficient to numerical tolerance. Significance continues to be assessed with the country-clustered fixed-effect p-value from equation (1) rather than from the bootstrap. For most outcomes matching leaves the adjusted and unadjusted contrasts nearly identical; surface water abstraction is the main exception, where conditioning on country and biome moves the counterfactual control level appreciably.

Finally, we conduct two complementary sensitivity analyses for unmeasured confounding variables (Supplementary Table C.3). First, we calculate E-values for the normalized difference of means with the *EValue* package in R[16]. E-values provide the minimum strength that an unmeasured confounder would need to have with both treatment assignment and the outcome, beyond the matched covariates, to fully explain away the observed effect[16]. Second, we compute Rosenbaum bounds, which assess how sensitive the matched-pair treatment effect is to a hypothetical violation of the assumption that matched units have equal probabilities of treatment assignment[17]. The critical Γ reports the maximum odds ratio of differential treatment assignment within matched pairs at which the conclusion of a significant effect would still hold. These diagnostics quantify sensitivity to unmeasured-confounding scenarios, but they do not rule out spatially structured confounding from governance, land tenure, enforcement, conflict, or pre-existing threat trajectories.

A.4 Species- and taxon-level estimation

We estimate species-level treatment effects on the composite threat index for threatened (VU, CR, EN) terrestrial vertebrates (mammals, amphibians, reptiles, and birds) by restricting the global matched sample to each species' geographic range (Supplementary Figure C.3). For coverage summaries, we use a raster-based overlap table recording, for each species s and protected area p, the number of 1-km cells shared by the species range and the PA, denoted a_{sp}, together with the species' total mapped range size. The species-level effect regressions instead use the rasterized species ranges to select matched pairs, as described below.

Pixel-level and PA-level treatment effects For each matched pair i, let

$$\delta_i = Y_i^{\text{treat}} - Y_i^{\text{control}}, \tag{3}$$

where Y_i^{treat} and Y_i^{control} are the composite threat values in the protected pixel and its matched control. For each protected area p, we then average these matched-pair differences over the n_p treated pixels belonging to that PA:

$$\delta_p = \frac{1}{n_p} \sum_{i \in p} \delta_i. \tag{4}$$

The PA-level standard error is defined as $\mathrm{sd}(\delta_i)/\sqrt{n_p}$ and the corresponding p-value is based on a two-sided t-test with $n_p - 1$ degrees of freedom. Only PAs represented in the matched sample receive a PA-level impact estimate. Species–PA overlaps are used only to calculate range coverage; neither PA-level impact estimates nor overlap weights enter the species-effect regressions or taxon medians.

Species-level estimation For each species s, we construct a species-specific matched sample by selecting all matched pairs whose PA pixels lie within the rasterized range of that species, and then retain both the PA and control observations from those pairs. Let $\mathcal{I}_s$ denote this sample. We estimate the species-level treatment effect from the regression

$$Y_i^s = \alpha + \delta_s T_i + \lambda_c + \mu_b + \varepsilon_i, \tag{5}$$

where Y_i^s is the composite threat index for observation i in the sample for species s, T_i indicates whether the observation is the protected pixel in the matched pair, λ_c denotes country fixed effects, and μ_b denotes biome fixed effects. The regression is estimated separately for each species s, so the intercept and fixed effects are species-specific. If the sample spans multiple countries and multiple biomes, both sets of fixed effects are included; when it spans multiple countries but only one biome, only country fixed effects are used; when it spans one country but multiple biomes, only biome fixed effects are used; and when neither varies, the regression is estimated without fixed effects.

The coefficient of interest is δ_s, which measures the average difference in the composite threat index between protected pixels in the species' range and their matched controls. When the species-specific sample spans more than one country, standard errors are clustered at the country level; otherwise heteroskedasticity-robust standard errors are used. If only one matched pair falls inside the species' range, the species effect is recorded as the difference between the PA and its control and no standard error is reported. Species with no matched pairs in range do not receive an estimated effect. We additionally compute the species-specific control mean, $\bar{Y}^{s,0}$, as the average composite threat index among control observations in $\mathcal{I}_s$. The species-level percentage effect is

$$\pi_s = 100 \times \frac{\delta_s}{\bar{Y}^{s,0}}, \tag{6}$$

expressing the treatment effect relative to the matched control mean within each species' range. We separately report the protected share of each species' mapped range as a descriptive coverage measure.

Taxon-level aggregation We summarize range-specific species effects at the taxon level using medians because percentage effects can be extreme when the species-specific matched-control mean is close to zero. Let $\mathcal{S}_\tau^\pi$ denote the set of species in taxon τ with a finite percentage effect from equation (6). The equal-weight taxon estimand is

$$\widetilde{\pi}_\tau = \text{median}_{s \in \mathcal{S}_\tau^\pi}(\pi_s)\,. \tag{7}$$

Thus, each contributing species receives equal weight within its taxon. For the level comparison in Fig. 5A, let $\mathcal{S}_\tau^L$ denote the species with finite matched-control levels and raw-scale effects. We separately summarize the species-specific matched-control level and implied protected level as

$$\begin{aligned} \widetilde{Y}_\tau^0 &= \text{median}_{s \in \mathcal{S}_\tau^L}\left(\bar{Y}^{s,0}\right), \\ \widetilde{Y}_\tau^1 &= \text{median}_{s \in \mathcal{S}_\tau^L}\left(\bar{Y}^{s,0} + \delta_s\right). \end{aligned} \tag{8}$$

These are separate marginal medians, so their difference need not equal the median species effect. We obtain uncertainty by resampling species with replacement within each taxon $B = 2{,}000$ times and recomputing each statistic. For any taxon median $\widetilde{\theta}_\tau$, the 95% percentile-bootstrap confidence interval is

$$\text{CI}_{0.95}\left(\widetilde{\theta}_\tau\right) = \left[Q_{0.025}\left(\left\{\widetilde{\theta}_\tau^{*(b)}\right\}_{b=1}^B\right), Q_{0.975}\left(\left\{\widetilde{\theta}_\tau^{*(b)}\right\}_{b=1}^B\right)\right]. \tag{9}$$

For the significance markers in Fig. 5A, we use the two-sided bootstrap sign probability for the median raw-scale effect δ_s. Biodiversity-weighted variants replace the ordinary median with a weighted median using terminal-branch-length, evolutionary-distinctiveness, or EDGE2 scores. Species with missing or non-positive weights are excluded from the corresponding weighted summary.

Global reference estimate For comparison, we also report the global mean PA-level effect obtained by weighting δ_p by the number of matched pixels in each PA:

$$\hat{\delta} = \frac{\sum_{p=1}^{P} n_p\, \delta_p}{\sum_{p=1}^{P} n_p}. \tag{10}$$

This is estimated via an intercept-only weighted least squares regression of δ_p on a constant with analytic weights n_p and standard errors clustered at the country level. Unlike the species and taxon summaries, this global reference estimate weights PAs by matched sample size rather than by species overlap.

A.5 Stochastic frontier analysis

The frontier analysis asks how low are the threat levels among the best-performing PAs that face similar matched-control pressure. The model is estimated with the *sfacross* function in the *sfaR* package[18]. Because lower within-PA threat levels are better, the frontier orientation is set to $S = -1$ and the lower envelope of the conditional distribution of $\bar{Y}_p^{\mathrm{PA}} = \delta_p + \bar{Y}_p^c$ traces the lower threat frontier implied by the data.

The main specification regresses the within-PA threat level on the control-side threat composite and lets the underperformance variance vary with PA size:

$$\bar{Y}_p^{\mathrm{PA}} = \beta_1\, \bar{Y}_p^c + \beta_2 \left(\bar{Y}_p^c\right)^2 + v_p + u_p, \qquad u_p \sim \mathcal{N}^+\left(0, \sigma_{u,p}^2\right), \quad \log \sigma_{u,p}^2 = \zeta_0 + \zeta_1 \log(\mathrm{size}_p + 1), \tag{11}$$

where $\bar{Y}_p^c$ is the mean composite threat in the matched control pixels of PA p, size_p is its area in km^2, $v_p \sim \mathcal{N}(0, \sigma_v^2)$ is symmetric noise, and $u_p \geq 0$ is the one-sided underperformance assumed half-normal with size-dependent dispersion. PA size is included as a determinant of performance variability rather than the frontier itself, reflecting the fact that smaller PAs tend to have noisier estimates, and this also ensures the frontier remains non-negative across all observed control threat levels. The variance share

$$\gamma = \frac{\overline{\sigma_u^2}}{\overline{\sigma_u^2} + \sigma_v^2}, \qquad \overline{\sigma_u^2} = \frac{1}{P} \sum_{p=1}^{P} \sigma_{u,p}^2,$$

summarizes the ratio of the averaged latent underperformance scale variance to total latent scale variance; in our main estimate $\overline{\sigma_u^2} = 0.004714$ and $\sigma_v^2 = 0.003637$, so that $\gamma = 0.5645$, with $\hat{\zeta}_1 = -0.325$ ($z = -23.7$), where underperformance dispersion in the smallest PAs is more than double that in the largest.

Two features of this summary are worth making explicit, because γ is easily over-read. First, the latent scale variances are averaged across PAs before the ratio is taken, so γ is not the average of PA-specific variance ratios. Second, γ is not the share of residual variance attributable to underperformance. Folding the latent normal variable onto the positive half-line reduces its dispersion, $\mathrm{Var}(u_p \mid \mathrm{size}_p) = (1 - 2/\pi)\, \sigma_{u,p}^2 \approx 0.363\, \sigma_{u,p}^2$, so the share of averaged conditional residual variance attributable to underperformance is instead

$$s_u^{\mathrm{Var}} = \frac{(1-2/\pi)\,\overline{\sigma_u^2}}{(1-2/\pi)\,\overline{\sigma_u^2} + \sigma_v^2} = 0.320.$$

The two summaries would coincide if u_p were an ordinary zero-mean normal variable; they differ here because u_p is half-normal.

For each PA we recover the underperformance term $\hat{u}_p$ from the conditional distribution of u_p given the composed residual $\hat{\varepsilon}_p = \bar{Y}_p^{\mathrm{PA}} - f(\bar{Y}_p^c; \hat{\beta})$, where $f(\cdot)$ is the fitted frontier of equation (11). Writing

$$\hat{\mu}_p^* = \frac{\hat{\sigma}_{u,p}^2}{\hat{\sigma}_{u,p}^2 + \hat{\sigma}_v^2}\,\hat{\varepsilon}_p, \qquad \left(\hat{\sigma}_p^*\right)^2 = \frac{\hat{\sigma}_{u,p}^2\,\hat{\sigma}_v^2}{\hat{\sigma}_{u,p}^2 + \hat{\sigma}_v^2}, \qquad z_p = \hat{\mu}_p^*/\hat{\sigma}_p^*,$$

the conditional-mean estimator is

$$\hat{u}_p = \mathbb{E}\left[u_p \mid \hat{\varepsilon}_p\right] = \hat{\mu}_p^* + \hat{\sigma}_p^*\,\frac{\phi(z_p)}{\Phi(z_p)}, \tag{12}$$

where ϕ and Φ are the standard normal density and distribution function. We then define the frontier value

$$\hat{Y}_{\min,p}^{\mathrm{PA}} = \bar{Y}_p^{\mathrm{PA}} - \hat{u}_p, \tag{13}$$

This is the model-implied lower within-PA threat frontier given the PA's counterfactual pressure. The PA-level frontier gap is $\hat{u}_p$ and the technical efficiency is $te_p = \exp(-\hat{u}_p)$.

Because PA size enters the underperformance variance, equation (12) weights the composed residual differently across PAs, and $\hat{u}_p$ is therefore a variance-weighted, truncation-adjusted quantity rather than the truncated raw residual $[\hat{\varepsilon}_p]_+$. The two are not interchangeable: since v_p may be negative, $\hat{u}_p > 0$ can hold even when $\hat{\varepsilon}_p < 0$, which is the case for 23.7% of PAs. We report $\hat{u}_p$ throughout and treat the truncated raw residual only as a descriptive diagnostic, because $\mathbb{E}\left[[u_p + v_p]_+ \mid u_p\right] > u_p$ whenever $\sigma_v > 0$: truncation retains positive noise while discarding negative noise, so symmetric noise no longer cancels in the aggregate and the resulting budget overstates underperformance.

Country-level aggregates are matched-pixel-weighted means of $\bar{Y}_p^{\mathrm{PA}}$, $\hat{Y}_{\min,p}^{\mathrm{PA}}$, and te_p. Because protected areas can straddle national borders, we do not attribute each PA to a single country. We instead construct an audited PA-by-country membership table from the matched pixels and replicate every PA across each country in which it holds matched pixels, weighting by that country's matched-pixel count and allocating the PA's reported area by the same shares, so that global pixel and area totals are preserved by construction. The crosswalk contains 22,284 PA–country memberships across the 22,090 protected areas in the frontier sample, of which 186 are transboundary, and yields the 107 country-level rows reported here.

We assess robustness in Extended Data Table B.3 by progressively saturating the deterministic frontier (columns 1–3: control level, quadratic, log-size) and then moving size from the deterministic frontier into the underperformance variance (column 4, the main specification).

Data availability

The source datasets analysed during this study are publicly available from the sources cited in the Methods and Supplementary Information. Derived analysis datasets can be shared by the corresponding author, subject to source-data license conditions and file-size constraints.

Code availability

The code used for this analysis will be archived in a public repository before publication.

Appendix References

1. UNEP-WCMC & IUCN. Protected planet: The world database on protected areas (WDPA) (2026). URL www.protectedplanet.net.
2. UNEP-WCMC. User manual for the world database on protected areas and world database on other effective area-based conservation measures: 1.6. Tech. Rep., UNEP-WCMC (2019). URL http://wcmc.io/WDPA_Manual.
3. Baylis, K. *et al.* Mainstreaming impact evaluation in nature conservation. *Conservation Letters* **9**, 58–64 (2016).
4. Salafsky, N. *et al.* A standard lexicon for biodiversity conservation: Unified classifications of threats and actions. *Conservation Biology* **22**, 897–911 (2008).
5. IUCN. The iucn red list of threatened species (2025). URL https://www.iucnredlist.org/en.
6. BirdLife International & Handbook of the Birds of the World. Bird species distribution maps of the world. version 2025.2. http://datazone.birdlife.org/species/requestdis (2025). Accessed on 25 February 2026.
7. IUCN. Species richness (spatial data). The IUCN Red List of Threatened Species. Version 2025-2. https://www.iucnredlist.org/resources/other-spatial-downloads (2025). Accessed on [DATE].
8. Ferraro, P. J. Counterfactual thinking and impact evaluation in environmental policy. *New Directions for Evaluation* **2009**, 75–84 (2009).
9. Geldmann, J., Manica, A., Burgess, N. D., Coad, L. & Balmford, A. A global-level assessment of the effectiveness of protected areas at resisting anthropogenic pressures. *Proceedings of the National Academy of Sciences* **116**, 23209–23215 (2019). URL https://pnas.org/doi/full/10.1073/pnas.1908221116.

10. Andam, K. S., Ferraro, P. J., Pfaff, A., Sanchez-Azofeifa, G. A. & Robalino, J. A. Measuring the effectiveness of protected area networks in reducing deforestation. *Proceedings of the National Academy of Sciences* **105**, 16089–16094 (2008). URL https://www.pnas.org/doi/abs/10.1073/pnas.0800437105. Publisher: Proceedings of the National Academy of Sciences.

11. Eklund, J. *et al.* Contrasting spatial and temporal trends of protected area effectiveness in mitigating deforestation in madagascar. *Biological Conservation* **203**, 290–297 (2016). URL https://linkinghub.elsevier.com/retrieve/pii/S0006320716305092.

12. Joppa, L. N. & Pfaff, A. High and far: Biases in the location of protected areas. *PLOS ONE* **4**, e8273 (2009). URL https://journals.plos.org/plosone/article?id=10.1371/journal.pone.0008273. Publisher: Public Library of Science.

13. Ribas, L. G. S., Pressey, R. L. & Bini, L. M. Estimating counterfactuals for evaluation of ecological and conservation impact: an introduction to matching methods. *Biological Reviews* **96**, 1186–1204 (2021).

14. Sekhon, J. S. & Grieve, R. D. A matching method for improving covariate balance in cost-effectiveness analyses. *Health Economics* **21**, 695–714 (2012).

15. Ho, D., Imai, K., King, G. & Stuart, E. MatchIt: Nonparametric preprocessing for parametric causal inference. *Journal of Statistical Software* **42**, 1–28 (2011).

16. VanderWeele, T. & Ding, P. Sensitivity analysis in observational research: introducing the e-value. *Annals of Internal Medicine* **167**, 268–274 (2017).

17. Rosenbaum, P. R. Observational studies. In Rosenbaum, P. R. (ed.) *Observational Studies*, 1–17 (Springer, 2002). URL https://doi.org/10.1007/978-1-4757-3692-2_1.

18. Dakpo, K. H., Desjeux, Y., Henningsen, A. & Latruffe, L. *sfaR: Stochastic Frontier Analysis Routines.* (2024). URL https://CRAN.R-project.org/package=sfaR/. R package version 1.0.1.

Acknowledgements

C.V. thanks the Italian Ministry of Education, University and Research, Programma Operativo Nazionale (CUP B85F21005360001) for funding her research activities.

Author contributions

C.V. and C.R. conceived the project. E.C. coordinated the modelling together with C.V., who both performed the data preparation and statistical analysis. All authors contributed to the manuscript preparation, led by C.V.

Competing interests

The authors declare no competing interests.

Additional information

Supplementary Information is available for this paper. Correspondence and requests for materials should be addressed to Claire Vincent.

B Extended Data

B.1 Extended Data Tables

Table B.1: **A description of the threat datasets used in this study and how they sit within the IUCN threat classification scheme.**

IUCN Threat Category	IUCN Threat Classification	Variable	Year	Dataset
1 Residential & commercial development	1.1–1.2 Residential & commercial development	Built-up area [m^2]	2020	Global Human Settlement Layer (GHS-BUILT-S R2023A) (Pesaresi & Politis, 2023)
2 Agriculture & aquaculture	2.1 Annual & perennial non-timber crops	Cropland [%]	2016–2019	Cropland extent (Potapov et al 2022)
	2.2 Wood & pulp plantations	Forest plantation [%]	2019	Global map of planting years (Du et al 2022)
	2.3 Livestock farming & ranching	No. of cattle [#]	2015	Gridded Livestock of the World v4 (GLW4; Gilbert et al 2018)
3 Energy production & mining	3.1 Oil & gas drilling	Oil & gas operation [%]	2020	Global Oil and Gas Extraction Tracker (Global Energy Monitor, 2022)
	3.2 Mining & quarrying	Mining operations [%]	2017	Global mining footprint (Tang & Werner 2023)
	3.3 Renewable energy	Renewable energy [%]	2020	Global Wind Power Tracker (Global Energy Monitor, 2023) & Global Power Plant Database (Global Energy Observatory, 2019)
4 Transportation & service corridors	4.1 Roads & railroads	Road presence [%]	2015	Global Roads Inventory Project (GRIP4) (Meijer et al 2018) & Global Railways dataset (WFP, 2019)
	4.2 Utility & service lines	Power lines presence [%]	2019	Global Power System (Arderne et al. 2020)
5 Biological resource use	5.1 Hunting & collecting terrestrial animals	*Not considered since no global map on hunting & collecting animals exists.*		
	5.3 Logging & wood harvesting	Forest loss 2001–2020 [area share]	2020	Forest cover change (Hansen et al. 2013)
6 Human intrusions & disturbance		*Not considered, since this is likely only mitigated in well-managed PAs (Kearney et al 2020).*		
7 Natural system modifications	7.1 Fire & fire suppression	Burned area [%]	2020	MODIS burned area products (Giglio et al 2018)
	7.2.1–7.2.4 Abstraction of surface water	Surface water use [% change]	2020	Global Surface Water Explorer (Pekel et al 2016)
	7.2.9–7.2.11 Dams	Dams presence [%]	2020	Global Georeferenced Database of Dams (GOODD; Mulligan et al 2020) & Global Power Plant Database (Global Energy Observatory, 2019)
8 Invasive & other problematic species, genes & diseases		*Not considered, since this is likely only mitigated in well-managed PAs or through landscape management and species control (Kearney et al 2020).*		
9 Pollution	9.6.1 Light pollution	Light intensity [DN]	2018	Harmonized global nighttime light (Li et al 2020)
10 Geological events		*Not considered, since this is likely only mitigated in well-managed PAs through restoration (Kearney et al 2020).*		
11 Climate change & severe weather		*Not considered, since this is likely only mitigated in well-managed PAs through restoration (Kearney et al 2020).*		
12 Other options		*Not considered.*		

Table B.2: **Difference in threat levels between protected areas and matched control sites.**

	Built area [m^2] (1)	Cropland [%] (2)	Forest plantation [%] (3)	No. of cattle (4)	Oil & gas operation [%] (5)
Protected area	−421.476**	−1.343***	0.016	−110.068*	−0.000
	(162.300)	(0.317)	(0.253)	(63.493)	(0.000)
Control mean	1035.307	3.156	1.814	520.022	0.000
Num. obs.	11,423,056	11,262,822	5,644,676	11,328,380	7,903,210
Num. countries	107	107	74	107	24
Adj. R^2	0.044	0.230	0.296	0.282	0.000

	Mining operations [%] (6)	Renewable energy presence [%] (7)	Road presence [%] (8)	Power lines presence [%] (9)	Burned area presence [%] (10)
Protected area	−0.089***	−0.010*	−0.865***	−0.880***	−0.010
	(0.034)	(0.005)	(0.220)	(0.237)	(0.063)
Control mean	0.127	0.019	6.120	3.016	0.369
Num. obs.	11,270,260	10,672,414	11,423,056	11,423,056	11,076,314
Num. countries	89	88	107	107	82
Adj. R^2	0.002	0.004	0.154	0.083	0.024

	Surface water change [% change] (11)	Dams presence [%] (12)	Light intensity [DN] (13)	Forest loss 2001–20 [m^2] (14)
Protected area	−1.159	0.001	−0.304*	−0.060***
	(1.336)	(0.003)	(0.178)	(0.020)
Control mean	−7.723	0.010	2.030	0.095
Num. obs.	342,974	11,347,846	11,423,056	4,577,994
Num. countries	90	101	107	87
Adj. R^2	0.104	0.001	0.211	0.077

	Any threat [%] (16)	Threat composite [0-1] (17)
Protected area	−0.072**	−0.018**
	(0.033)	(0.007)
Control mean	0.485	0.058
Num. obs.	11,423,056	11,423,056
Num. countries	107	107
Adj. R^2	0.289	0.227

Note: The global average treatment effect on protected areas (ATT) for each of the 14 individual threat indicators, the any-threat indicator, and the composite threat index. Each column is a separate OLS regression with country and biome fixed effects. Standard errors clustered at the country level in parentheses. */ **/ *** denote $p < 0.1/0.05/0.01$, respectively.

Table B.3: **Stochastic frontier estimation results.**

	(1) Control	(2) + Quadratic	(3) + Size	(4) Main: uhet
Frontier coefficients				
Control threat level	0.6899***	0.4907***	0.4004***	0.3558***
	(0.004 0)	(0.009 3)	(0.008 2)	(0.007 4)
Control threat level^2		0.3930***	0.4650***	0.5533***
		(0.016 5)	(0.014 5)	(0.013 5)
log(PA size + 1)			−0.0048***	
			(0.000 3)	
σ_u eq.: intercept	−7.5233***	−6.2019***	−5.1437***	−4.6219***
	(0.115 5)	(0.062 7)	(0.024 8)	(0.024 7)
σ_u eq.: log(PA size + 1)				−0.3250***
				(0.013 7)
Variance parameters				
σ_u	0.0232	0.0450	0.0764	0.0687
σ_v	0.0754	0.0707	0.0586	0.0603
γ	0.087	0.288	0.629	0.564
Log-likelihood	25 355.5	25 428.6	25 646.8	25 873.1
AIC	−50 705.1	−50 849.3	−51 283.6	−51 736.3
N (PAs)	22,090	22,090	22,090	22,090
Mean efficiency	0.982	0.965	0.943	0.950
Median gap	0.0180	0.0325	0.0493	0.0410

Note: The dependent variable is the PA-level mean within-PA threat composite, so the frontier is a model-implied minimum threat level given counterfactual pressure. Columns (1)–(3) progressively add the control-side threat level, its square, and $\log(\text{PA size} + 1)$ to the frontier. Column (4), the main specification, moves $\log(\text{PA size} + 1)$ to the underperformance variance to ensure the frontier remains non-negative across all observed pressure levels. σ_u and σ_v are latent scale standard deviations. γ is the ratio of the averaged latent underperformance scale variance to total latent scale variance. * $p < 0.1$, ** $p < 0.05$, *** $p < 0.01$. Standard errors in parentheses.

733
B.2 Extended Data Figures

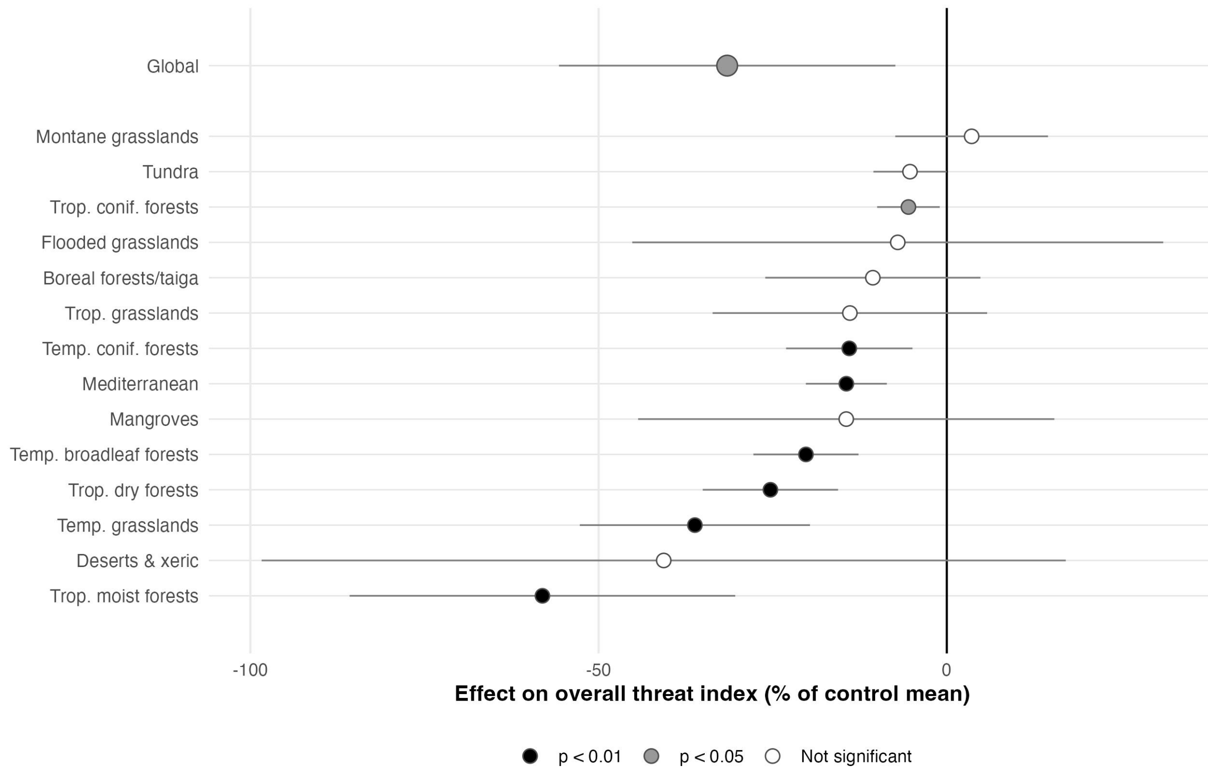

Figure B.1: **Effects of protected areas by biome.** Normalized treatment effect on the overall threat composite index by terrestrial biome, expressed as percentage of the control group mean. Point estimates with 95% confidence intervals. Standard errors are clustered at the country level. See Supplementary Table C.5 for biome-level protection shares and Supplementary Table C.6 for threat-specific estimates.

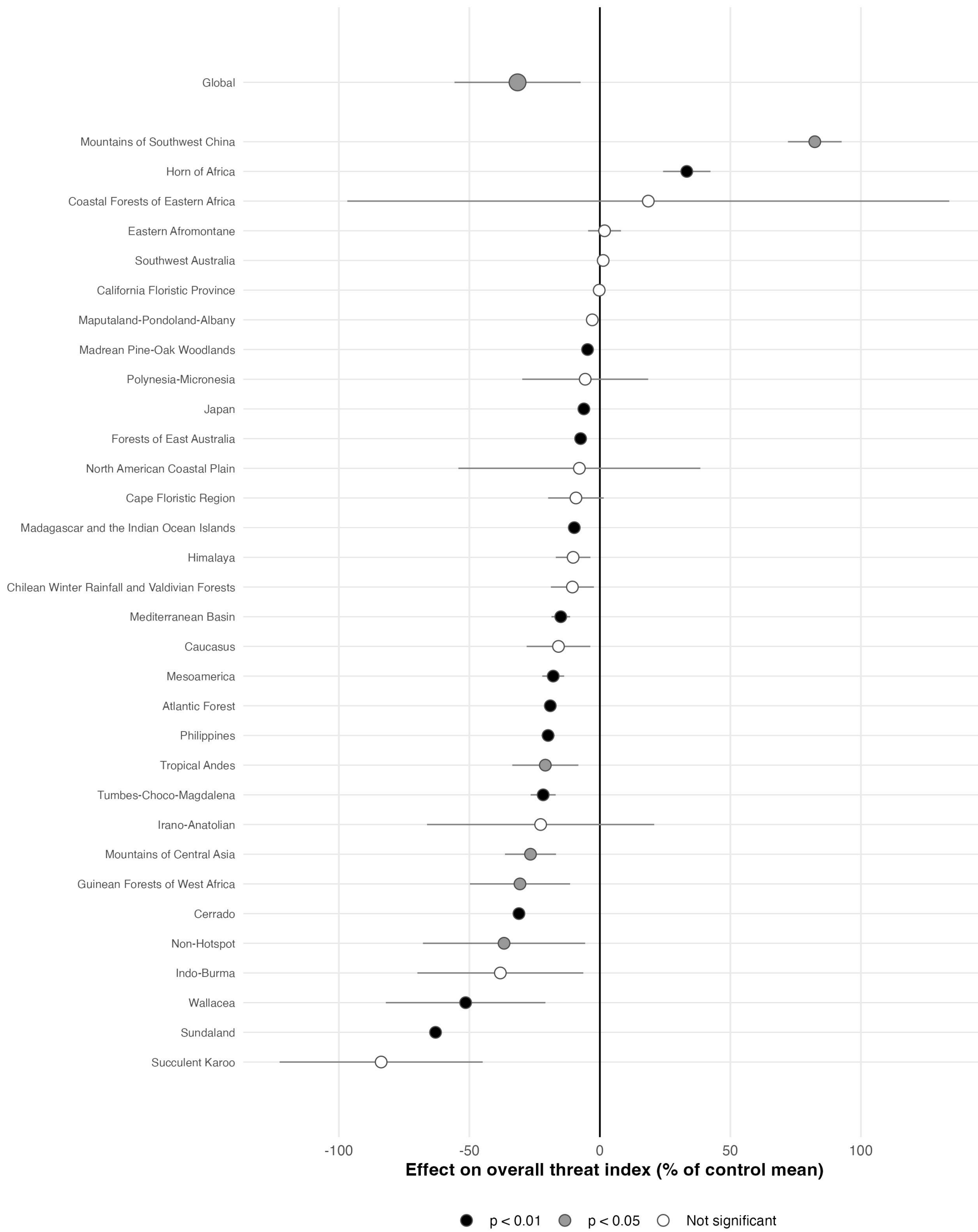

Figure B.2: **Effects of protected areas by biodiversity hotspot.** Normalized treatment effect on the overall threat composite index for each of the 31 biodiversity hotspots represented in the matched sample and for the non-hotspot remainder, expressed as a percentage of the control group mean. Point estimates with 95% confidence intervals. Regressions include country and biome fixed effects with standard errors clustered at the country level, falling back to the varying dimension alone where a hotspot spans a single country or a single biome. The global estimate is shown at the top for reference.

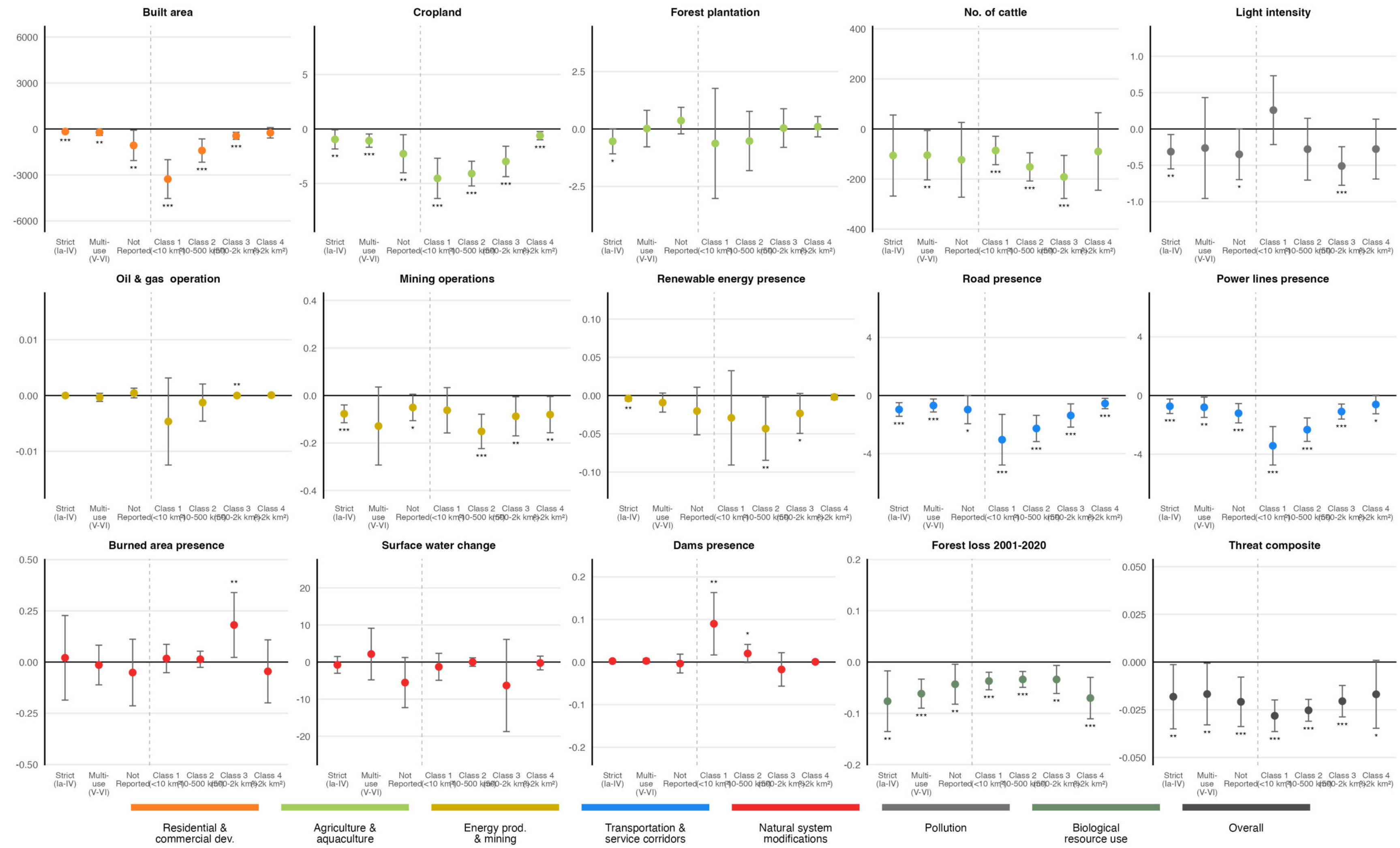

Figure B.3: **Effects by protected area characteristics.** Average treatment effects on the treated (ATT) estimated separately by IUCN management category (Strict: Ia–IV, Multi-use: V–VI, Not Reported) and PA size class (Class 1: <10 km^2, Class 2: 10–500 km^2, Class 3: 500–2000 km^2, Class 4: >2000 km^2). Point estimates with 95% confidence intervals. All regressions include country fixed effects with standard errors clustered at the country level. */ **/ *** denote $p < 0.1/0.05/0.01$, respectively.

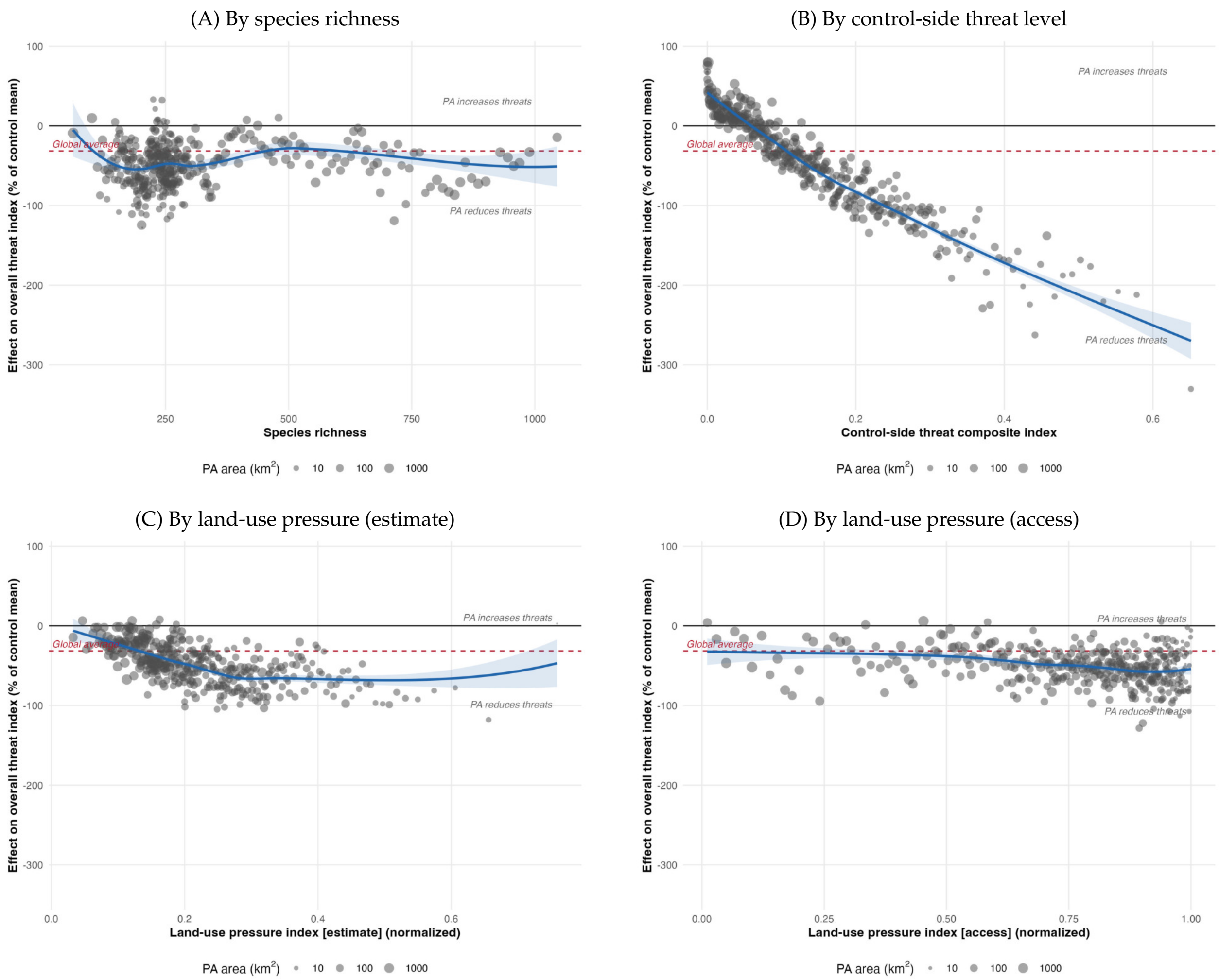

Figure B.4: **PA-level heterogeneity in threat reduction.**PA-level threat reductions (as % of global control mean) plotted against (a) species richness, (b) the composite threat level of the matched controls, (c) land-use pressure, and (d) accessibility. Each point represents the mean across 400 equal-count bins of PAs, sized proportionally to mean area. Blue lines show loess smoothers with 95% confidence intervals (shading), the dashed red line indicates the global average treatment effect. Negative values indicate PAs that reduce threats relative to matched controls.

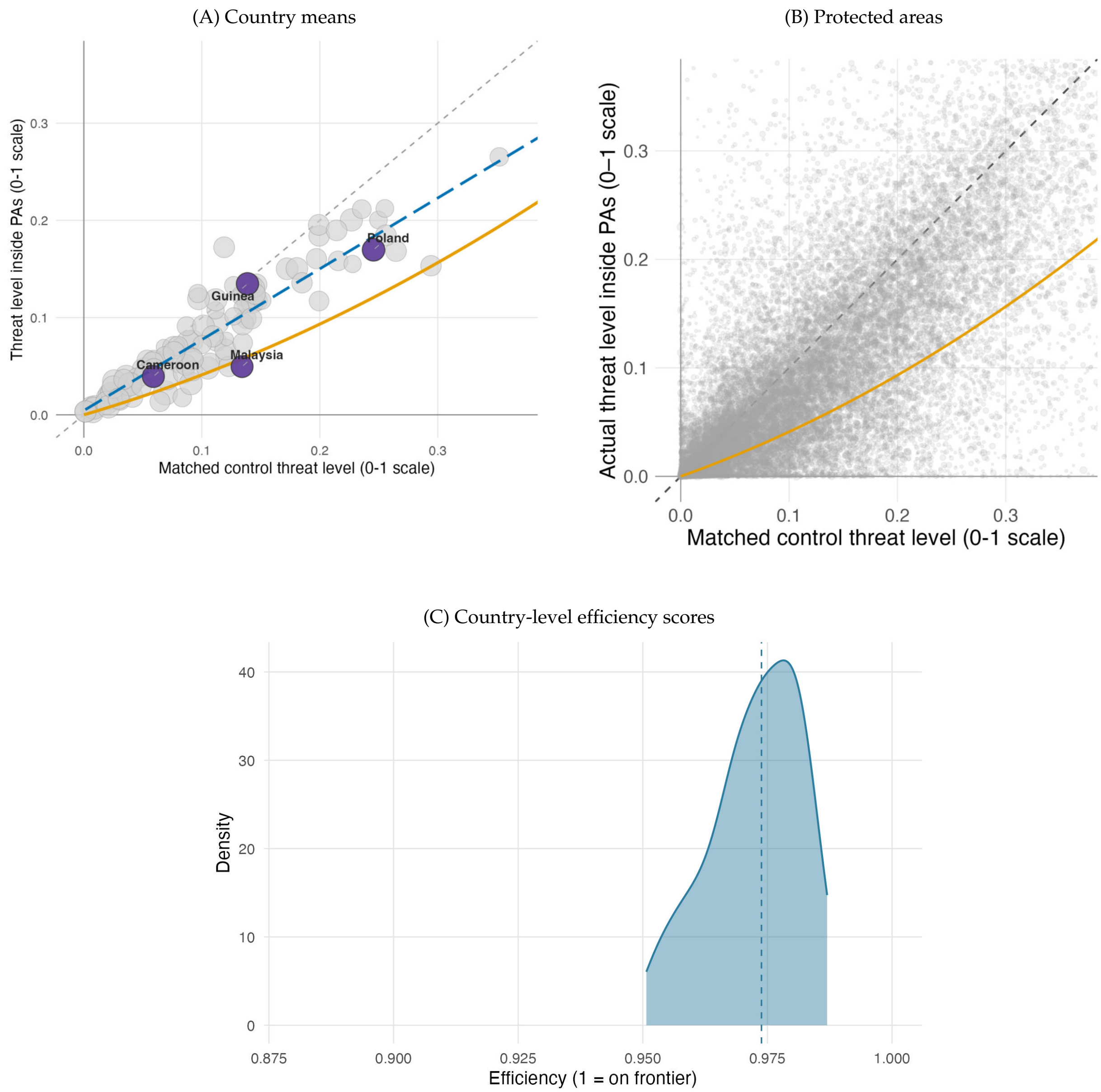

Figure B.5: **Observed threat reduction and frontier benchmarks across countries and PAs.** Stochastic frontier analysis (a) aggregated to the country level, and (b) individual PAs, with the fitted minimum-threat frontier (orange curve), the OLS-model fit (blue dashed line), and equal threat inside and outside PAs (the grey dashed line). (c) The distribution of country-level efficiency scores (1 = on-frontier), with the dashed vertical line marking the median.

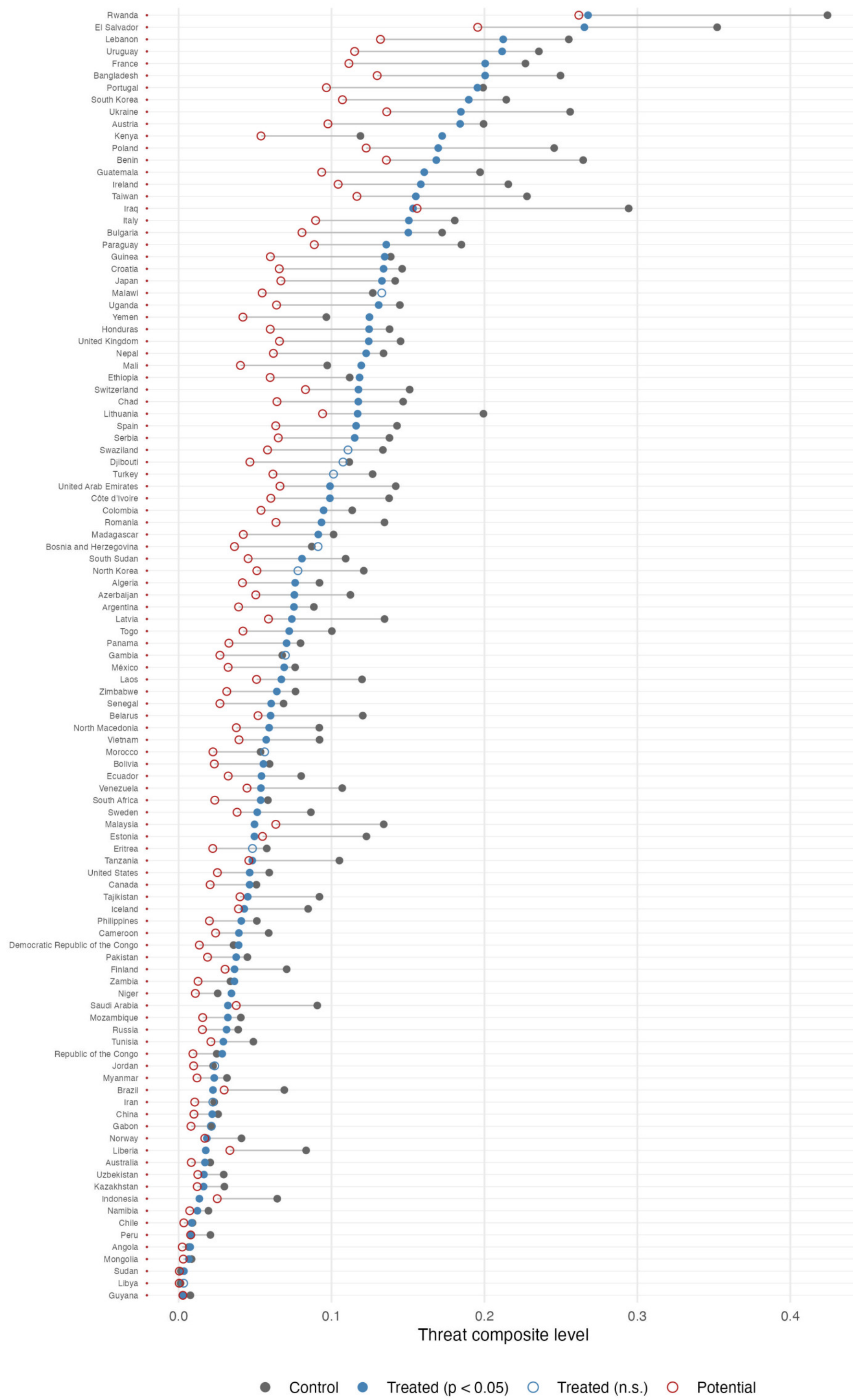

Figure B.6: **National threat levels and performance gaps.** Country-level threat reduction and performance gap from stochastic frontier analysis. Each row shows a country's matched control threat level (grey), observed threat level inside PAs (blue; filled if significant at p<0.05), and the minimum-threat frontier given counterfactual pressure (red). The horizontal distance between the observed PA level and the frontier is the estimated performance gap. The frontier captures performance relative to observed best practice under comparable pressure, not the magnitude of threat reduction alone.

C Supplementary Information

C.1 Data description and processing

C.1.1 Threat outcomes

We use publicly available global pressure maps that correspond to fourteen spatial threat indicators mapped to the IUCN Red List threat classification scheme (Extended Data Table B.1)[6]. Maps at different resolutions are resampled to 1 km^2 resolution and reprojected to Mollweide equal-area projection in GRASS GIS v8.3.

Residential & commercial development (Threats 1.1–1.2) We used the Global Human Settlement Layer (GHS-BUILT-S - R2023A)[2] which maps built-up surfaces derived from Sentinel2 and Landsat data from 2020 at 1 km^2 resolution.

Annual & perennial non-timber crops (Threat 2.1) We use the global cropland extent raster from 2016 to 2019[3] and calculate the percentage fraction of cropland within each grid cell.

Wood & pulp plantations (Threat 2.2) We use a global raster map of planting years with 30-meter spatial resolution[4]. We aggregated this map to our 1 km^2 grid where each cell that included a plantation established between 2015 and 2019 is given a value of 1.

Livestock farming & ranching (Threat 2.3) We use the Gridded Livestock of the World v4 dataset (GLW4)[5], which provides a modeled livestock distribution in 2015 at a resolution of 30 arc-seconds (approximately 1 km at the equator). We aggregated the livestock map to our 1 km^2 grid by taking the maximum pixel value within each grid cell.

Oil & gas drilling (Threat 3.1) We use the Global Oil and Gas Extraction Tracker dataset[6] which contains vectorized location points with information on the production start year between 1934 and 2020. We rasterize the data to the 1 km^2 grid cells after removing "discovered" sites and those without exact coordinates.

Mining & quarrying (Threat 3.2) We rasterize the global mining footprint of 2017 map[7], where pixels overlapping the mining footprint area are assigned a value of 1 and all other pixels are 0.

Renewable energy (Threat 3.3) We combine the Global Wind Power Tracker data[8] and the renewable energy types extracted from the Global Power Plant Database[9], which included geothermal power production, solar farms, wind farms, and tidal farms. Dams were excluded from this dataset as they are addressed separately under Threat 7.2.9.

Roads & railroads (Threat 4.1) We use a combination of the Global Roads Inventory Project (GRIP4)[10] and the Global Railways dataset[11] for 2015. These vector datasets were rasterized to 1 km^2 grid cells whereby cells overlapping with the original vector lines have a value of 1.

Utility & service lines (Threat 4.2) We use the Global Power System map[12] providing data from 2015 to 2019. We assign the value of 1 to grid cells that overlap with power lines, and a value of 0 if not.

Logging & wood harvesting (Threat 5.3) We use the forest loss dataset at 30-meter resolution from the Global Forest Change 2000–2024[13]. We considered pixels as having lost forest if they had a forest cover greater than 90% in 2000, and were identified as having lost forest cover in 2020. We then aggregated the data to our 1 km^2 grid using a weighted-sum. Note: datasets to meaningfully investigate hunting & collecting terrestrial animals (Threat 5.1) at a global scale are not available.

Fire & fire suppression (Threat 7.1) We used the MODIS monthly burned area products from January and June 2020[14]. Pixels are assigned a value of 1 if they were burned in either month.

Abstraction of surface water (Threats 7.2.1–7.2.4) We use the Global Surface Water Explorer[15] which tracks surface water changes from 2000 to 2020 at 30-metre resolution. We create a map for 2020 with values ranging from -100 to 99, where lower values indicate greater surface-water loss since 2000, higher values indicate gains, and 0 indicates no net change. We aggregated the data by taking the average value per grid cell.

Dams (Threats 7.2.9–7.2.11) We combine the Global Georeferenced Database of Dams (GOODD)[16] with dams from the Global Power Plant Database[8], assigning a value of 1 to grid cells containing dams.

Light pollution (Threat 9.6.1) We derive a light pollution map based on the harmonized global nighttime light dataset[17] for 2018 with a spatial resolution of 30 arc-seconds (approximately 1 km at the equator). Each pixel was assigned a radiance value ranging from 0 to 63 DN, with higher values indicating greater light intensity.

Any threat (indicator) We construct a binary composite indicator that equals one if any of the 14 individual threats is classified as present at a given pixel, and zero otherwise. Most threats are coded as present when their value is strictly positive (i.e., any non-zero value). Three exceptions use quantile-based thresholds computed from the full unmatched sample. Pasture is coded as present only above the 75th percentile of livestock density, light pollution only above the 75th percentile of nighttime radiance, and surface water abstraction only below the 25th percentile, since lower values indicate greater water loss. This variable captures the extensive margin of overall threat exposure regardless of threat type.

Overall threat composite We construct a continuous composite index that summarizes the overall intensity of all threats at each pixel on a $[0, 1]$ scale. The index aggregates the 14 individual threat indicators through a hierarchical weighting scheme that mirrors the IUCN threat classification and accounts for cross-country differences in threat prevalence.

Step 1: Global normalization. Each threat indicator k is normalized to $[0, 1]$ using winsorized min-max scaling based on the 1st and 99th percentiles computed across the full global unmatched sample:

$$\tilde{Y}_{ik} = \frac{Y_{ik} - P_k^1}{P_k^{99} - P_k^1}, \tag{14}$$

where P_k^1 and P_k^{99} are the global 1st and 99th percentiles of threat k. Normalized values are clipped to $[0,1]$. The surface water abstraction indicator is inverted $(1-\tilde{Y}_{ik})$ so that higher values consistently indicate greater threat intensity. For sparse threats where $P_k^1 = P_k^{99}$ (i.e., the variable is zero at both percentiles), the normalized value is set to one if the threat is classified as present at the pixel and zero otherwise, using the same presence thresholds described above.

Step 2: Country-level prevalence weights. For each threat k in country c, we compute the share of pixels where the threat is present, $\bar{w}_{kc} = \frac{1}{N_c}\sum_{i\in c}\mathbf{1}[Y_{ik}\text{ exceeds threshold}]$, using the same presence thresholds as for the *any threat* indicator. Within each IUCN category $\mathcal{C}$, these prevalence shares are normalized to sum to one:

$$\alpha_{kc} = \frac{\bar{w}_{kc}}{\sum_{\ell\in\mathcal{C}}\bar{w}_{\ell c}}. \tag{15}$$

If no threat in a category is present in a country, that category receives no weight for that country.

Step 3: Category-level aggregation. The 14 threats are grouped into seven IUCN threat categories $\mathcal{C}$: residential & commercial development, agriculture & aquaculture, energy production & mining, transportation & service corridors, biological resource use, natural system modifications, and pollution (Extended Data Table B.1). For single-threat categories, the category index equals the normalized value. For multi-threat categories, the index is the prevalence-weighted average of the normalized threats within the category:

$$I_{i,\mathcal{C},c} = \sum_{k\in\mathcal{C}}\alpha_{kc}\,\tilde{Y}_{ik}. \tag{16}$$

Step 4: Overall composite. The threat composite is the average of the active category indices:

$$Y_{ic}^{\text{comp}} = \frac{1}{|\mathcal{A}_c|}\sum_{\mathcal{C}\in\mathcal{A}_c} I_{i,\mathcal{C},c} \tag{17}$$

where $\mathcal{A}_c$ is the set of IUCN categories with positive prevalence in country c. Pixels in countries where all prevalence weights are zero receive a missing value. This hierarchical weighting ensures that each IUCN threat category contributes to the composite as a group rather than being dominated by the number of individual indicators it contains, and the index reflects country-specific threat profiles within each category, giving more weight to threats that are prevalent in a given country. The final country-specific contribution weights, $\alpha_{kc}/|\mathcal{A}_c|$, are summarized in Supplementary Information Fig. C.2.

C.2 Matching covariates

Agricultural suitability The highest agro-climatic potential yield (estimated from historical climatic conditions 1971-2000) per pixel[18] of 16 crops that are most important for the global economy, food security and biofuels[19]; *Hordeum vulgare, Manihot esculenta, Arachis hypogaea, Zea mays, Pennisetum americanum, Elaeis guineensis, Solanum tuberosum, Brassica napus, Oryza sativa, Secale cereale,* *Sorghum bicolor, Glycine maximum, Saccharum officinarum, Helianthus annus, Triticum aestivum,* and *Triticum gestivum*. Resolution of 5 arcminutes (about 9x9 km at the equator). Previous studies have found that the establishment of protected areas coincided with low-productivity lands unsuitable for agriculture[20,21]. Both old and new protected areas do not target places with high concentrations of threatened vertebrate species but instead were established in locations that minimize conflict with agriculturally suitable lands[22].

Precipitation Total annual precipitation calculated with the sum of 12 months precipitation data[23]. Each month was derived from the average monthly precipitation data for 1970-2000. From WorldClim version 2.1 released in January 2020 with a resolution of 30 arcseconds (about 1x1 km at the equator). Precipitation has a very strong link to agricultural suitability. Additionally, temperature and precipitation are the most critical factors that control the distribution of species in terrestrial ecosystems[24,25].

Temperature Average annual temperature calculated from monthly mean temperature data for 1970-2000[23]. From WorldClim version 2.1 released in January 2020 with a resolution of 30 arcseconds. Temperature has a very strong link to agricultural suitability. Additionally, temperature and precipitation are the most critical factors that control the distribution of species in terrestrial ecosystems[24,25].

Human population density The Gridded Population of the World, Version 4 (GPWv4), for the year 2000 with a resolution of 30 arcseconds[26]. Human population density is a key cause of species becoming threatened with extinction and continued increase in human population densities increases species biodiversity threats[27]. The establishment of protected areas coincided with wild and scenic areas far from human activity[21].

Travel time Estimated travel time to the nearest city of 50,000 or more people in the year 2000, with pixel values representing minutes of travel time with a resolution of 30 arcseconds[28]. Remoteness is an underlying characteristic of highly threatened protected areas, and the number of threats was lower in more remote protected areas[29]. Most protected areas are biased to places with greater distances to roads and cities[24], and the establishment of protected areas coincided with wild and scenic areas far from human activity[21,20].

Biome We included all 14 terrestrial biomes[39]. This vector data was rasterized to 1x1 km grid cells and included in the matching algorithm as an exact match. The global pattern of protected area coverage is influenced by vertebrate biodiversity, human activities and agricultural suitability, however the relative importance of these factors varies among biogeographical realms[32]. There is also a difference between forested and non-forested protected areas in their ability to mitigate anthropogenic threats[33].

Country Country boundaries. This vector data was rasterized to 1x1 km grid cells and included in the matching algorithm as an exact match. The number of reported threats is lower in protected areas with higher control of corruption and lower human development scores[29], which can vary greatly between countries. *Source:* Natural Earth v5.1.1

Elevation Global digital elevation model (GTOPO30) from USGS with a resolution of 30 arcseconds[34]. Protected areas are preferentially placed in higher elevations[21,24]. Additionally, protected areas at higher elevations have fewer reported threats[29].

Slope Slope was calculated from the above digital elevation model in GRASS GIS using the r.slope.aspect function. Protected areas are biased to areas with steeper slopes[20,24]. *Source:* Own analysis

Tree cover Percentage tree cover in the year 2000 at 30-meter resolution[13], aggregated to 1 km^2 grid cells. Forest cover is a key determinant of protected area placement, as many PAs are established specifically to protect forested ecosystems. Additionally, tree cover influences the types and intensity of anthropogenic threats that may occur in an area, with forested regions facing distinct pressures such as logging and agricultural conversion compared to non-forested lands.

C.3 Protected area data

Data grid and protected area treatments The analysis is based on a 1x1 km grid over the global terrestrial area. A grid cell is labelled as treated when covered by a PA that was designated between 2001 and 2020. We use the February 2026 version of the World Database on Protected Areas (WDPA) and the World Database on Other Effective Area-based Conservation Measures[35], retaining national, regional, and international terrestrial sites. We exclude PAs smaller than 1 km^2 to reduce confounding effects of control and treatment areas within the same pixel. We also removed UNESCO-MAB Biosphere Reserves from the WDPA because these sites include a buffer and transition zone that, in many cases, do not act as PAs[36]. PAs without a recorded boundary are stored as points in the WDPA, and these were excluded from the analysis. Some countries choose to restrict their data by making it unavailable to the public. To account for this, the 2016 version of the WDPA is added for China, Estonia, India, and Turkey when the spatial information for their PAs was still publicly available.

For areas where PAs overlap, we retain a single protected-area identifier by ordering polygons by designation year before rasterization. Each grid cell then inherits the selected protected area's IUCN Protected Area Management Category and reported area. We classify PAs as strictly protected (IUCN categories Ia–IV) or multi-use (IUCN categories V and VI) and categorize PAs into four bins according to their size: less than 10 km^2, 10-500 km^2, 500-2000 km^2, and over 2000 km^2.

Control units are grid cells that do not intersect with any PA in the WDPA and the WD-OECM network. To avoid potential estimation biases from spatial leakages or positive spillovers[19], we further removed all areas within a 5 km buffer around PAs from potential control points. The final map was rasterized to 1x1 km cells in GRASS GIS v8.3.

Sample The initial dataset comprises approximately 136.7 million grid cells. We remove cells that cannot be assigned to a country and apply country-level restrictions to ensure data quality and comparability. We exclude Small Island Developing States and small island territories, countries where at least 30% of grid cells lack biodiversity data, and countries with a mean biodiversity index below 15. We then remove treated pixels associated with PAs of at most 1 km^2, point-derived PA records, and UNESCO-MAB Biosphere Reserves. These rules yield an unmatched matching input of 127,314,386 grid cells across 157 countries. Matching produces 6,064,399 pairs across 145 countries before country-level balance filtering, and the final analysis sample comprises 5,711,528 matched pairs across 107 countries and 22,090 PAs.

C.4 Biodiversity and land-use pressure variables

Threatened species ranges We retrieved data on the number of threatened vertebrate species (mammals, reptiles and amphibians) from the IUCN Red List version 2025-1[38]. We included all species assessed on the global Red List that are threatened with extinction (i.e. Vulnerable, Endangered, and Critically endangered species) and contain geographical range data. We included threatened bird range data from the Birds of the World dataset[39]. The resulting dataset had a total of 7,165 species, of which 2,900 amphibians, 1,234 birds, 1,355 mammals, and 1,676 reptiles. We measure pixel-level species richness as the pixel-level threatened-species counts from the rasterized species range maps.

Total species richness We used an estimate of species richness per pixel for Extended Data Fig. B.4 Panel A based on the raw IUCN ranges for amphibians, birds, mammals and reptiles. This includes species with range information from all Red List categories and is based on the Red List version 2024-2[40].

Land-use pressure (estimated) The primary pressure index is a model-based measure that captures the expected intensity of threats at each pixel given its geographic and socioeconomic characteristics. It is constructed in two stages.

Stage 1: Threat-specific models. For each of the 14 individual threat outcomes $k \in \{1, \ldots, 14\}$, we fit a regression model on all control pixels using the eight matching covariates as predictors:

$$g\big(\mathbb{E}[y_{ik}]\big) = \alpha_k + \boldsymbol{x}_i' \boldsymbol{\beta}_k, \tag{18}$$

where y_{ik} is the observed value of threat k at pixel i, $\boldsymbol{x}_i$ is the vector of matching covariates, and $g(\cdot)$ is the link function. For non-negative outcomes, we use a Poisson regression (log link, $g = \ln$); for surface water abstraction that takes negative values, we use OLS (identity link, $g = \text{id}$).

Stage 2: Aggregation. We compute fitted values $\hat{y}_{ik}$ for *all* pixels (both PA and control). Each threat-specific prediction is then normalized to $[0, 1]$ using the global min-max range across all pixels:

$$\tilde{y}_{ik} = \frac{\hat{y}_{ik} - \min_j \hat{y}_{jk}}{\max_j \hat{y}_{jk} - \min_j \hat{y}_{jk}}. \tag{19}$$

The estimated land-use pressure index is the mean of the normalized predictions across all 14 threats:

$$P_i^{\text{est}} = \frac{1}{14} \sum_{k=1}^{14} \tilde{y}_{ik}. \tag{20}$$

For Extended Data Figure B.4 panel C, this index is further normalized within each country using min-max scaling, analogous to the biodiversity variable.

Land-use pressure (accessibility) A minimal pressure proxy defined as inverted travel time: $P_i^{\text{access}} = 1 - \tilde{x}_i^{\text{access}}$, where $\tilde{x}_i^{\text{access}}$ is the min-max normalized travel time to the nearest city of 50,000+ inhabitants[28], normalized across all pixels. Higher values indicate greater accessibility and, by extension, higher anthropogenic pressure. This index is subsequently normalized within each country.

C.5 Supplementary Methods

Table C.1: Matching diagnostics: covariate balance and multicollinearity

	Std. mean difference			Variance ratio			VIF	
Predictor variable	Unmatched	Matched	% impr.	Unmatched	Matched	% impr.	Unmatched	Matched
Elevation	−0.188	0.002	99	0.534	1.009	99	1.43	1.53
Population 2000	−0.132	0.000	100	0.111	1.066	97	1.02	1.01
Precipitation	0.361	0.011	97	1.457	1.026	93	2.18	4.11
Slope	−0.029	0.011	62	1.039	1.070	−79	1.42	1.60
Temperature	0.352	−0.003	99	0.848	1.000	100	3.64	3.76
Access	0.353	0.052	85	0.930	1.105	−39	1.29	1.30
Crop suitability	0.068	−0.002	98	0.826	1.005	97	3.52	3.45
Forest cover 2000	0.562	0.010	98	2.856	1.016	99	1.71	3.53

Note: The table reports covariate balance and multicollinearity diagnostics for the eight continuous matching covariates. Standardized mean differences (SMD) use the pooled pre-matching standard deviation as the denominator. Variance ratios compare treated and control variance. Percentage improvement reports the reduction in absolute imbalance after matching. Variance inflation factors (VIF) are computed before and after matching on random subsamples of 200,000 observations; biome and country are excluded because they are exact-match categorical variables. A VIF below 5 is interpreted as low multicollinearity risk.

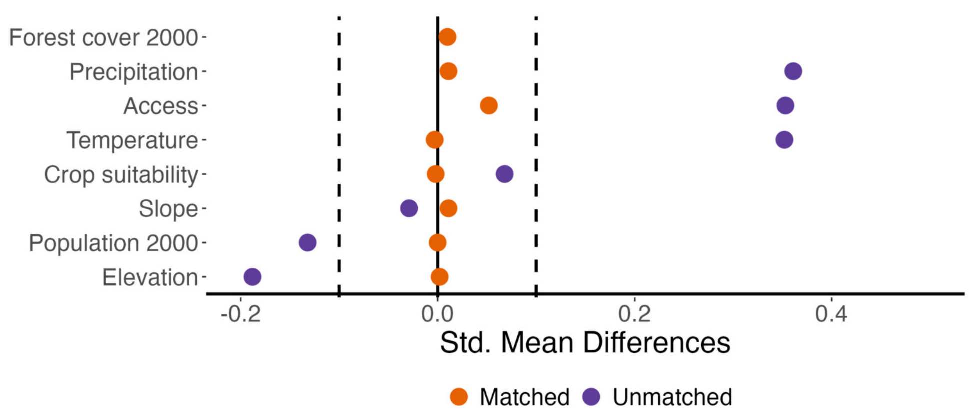

Figure C.1: **Assessing matching quality.** Covariate balance showing the standard mean differences of covariates before (purple) and after (orange) Mahalanobis matching. To determine imbalance, we used a threshold of >0.1 (dashed lines). See Table C.1 for detailed balance and VIF statistics.

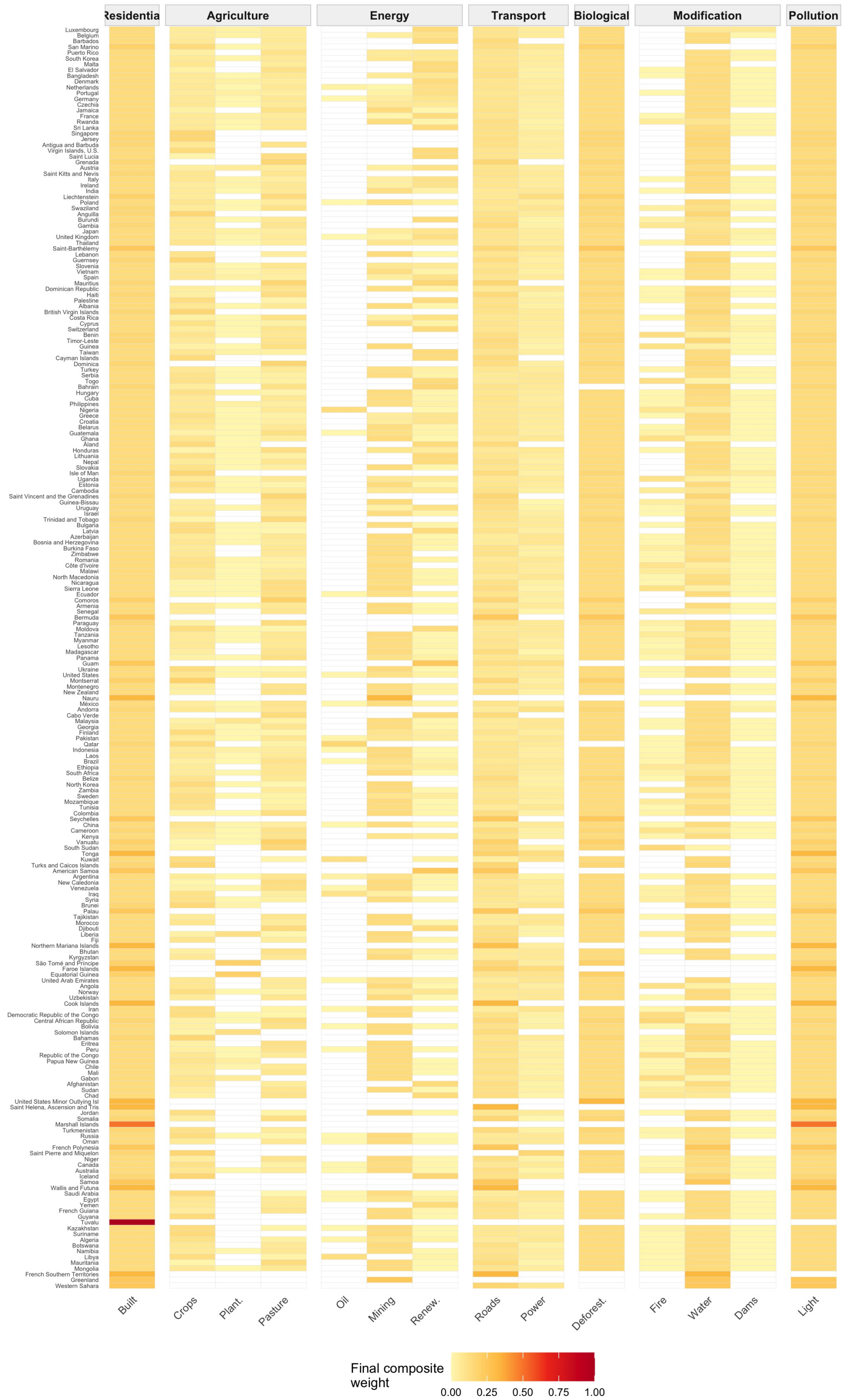

Figure C.2: **Final country-specific prevalence weights used in the threat composite.** Each cell reports the final country-specific contribution weight applied to the corresponding normalized threat in the composite index. Weights sum to one across all displayed threats for each country with at least one active category, and white cells indicate zero weight. Rows are ordered by the total raw prevalence across all 14 threats.

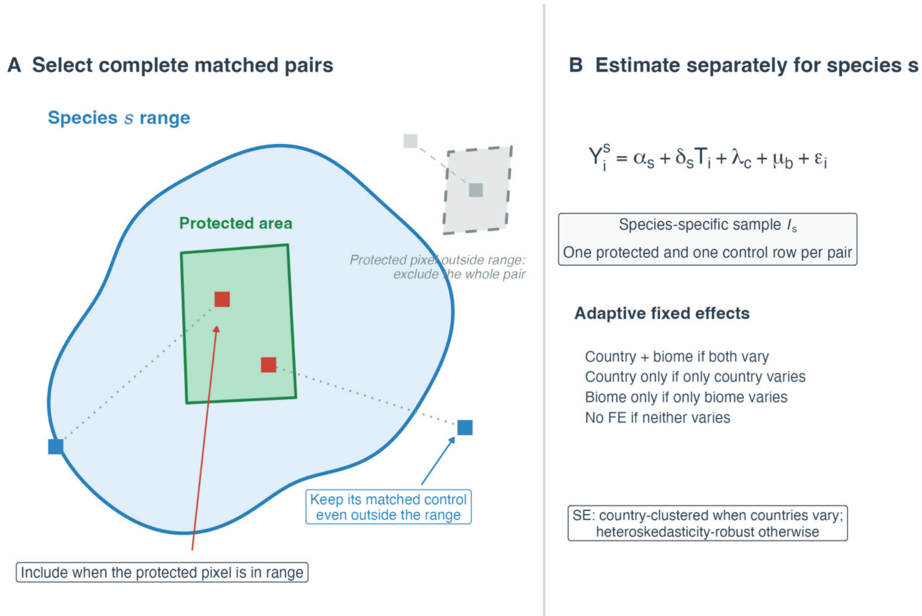

Figure C.3: **Schematic illustration of species-level estimation.** For each species s, matched pairs whose treated pixel (red) falls within the species' geographic range are selected along with their matched control pixel (blue) regardless of their overlap with the species range. Protected areas fully inside the range contribute all their matched pairs, and those that partially overlap contribute only pairs from the overlapping portion. Protected areas outside the range are excluded. Different species have different ranges and therefore draw on different subsets of matched pairs.

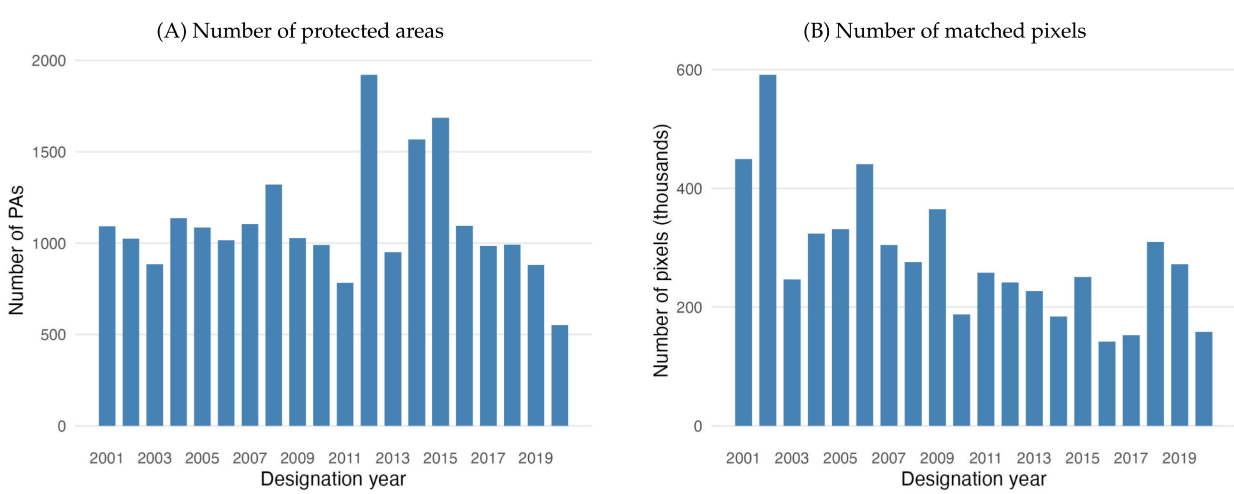

Figure C.4: **Matched sample composition by PA designation year.** Distribution of the matched treated sample by PA designation year (2001–2020), (a) by the number of distinct protected areas, (b) and by the number of treated 1 km^2 grid cells.

C.6 Additional analyses: Robustness tests

Sequential fixed effects and controls. Table C.2 shows that the global ATT on the threat composite is stable across alternative model specifications: from no fixed effects to country and biome fixed effects, with and without the eight matching covariates as additional controls, with PA-level fixed effects, with Conley spatial standard errors on a 10% subsample, and under a fractional-logit specification.

Sensitivity to unobserved confounding. Table C.3 reports E-values for the normalized mean difference between PA and control pixels and Rosenbaum-bound critical Γ values for each threat outcome. Both quantify the strength of unmeasured confounding needed to overturn the estimated effect.

Random subsampling and alternative matching. Figure C.5 shows the global ATT under (i) random 20% and 10% subsamples of the matched data, (ii) the production matching procedure on a stratified 1% subsample of the unmatched data, and (iii) alternative matching procedures applied to the same 1% subsample (parsimonious vs. expanded covariates, 1:2 and 1:5 ratios, with and without replacement, propensity-score matching with and without caliper, coarsened exact matching).

Table C.2: Robustness: Sequential addition of fixed effects and controls

	(1) Unmatched	(2) Unmatched + FE	(3) No FE	(4) Country FE	(5) Country + Biome	(6) + Controls	(7) + PA FE	(8) Conley SEs	(9) Frac. logit
Protected area	−0.050***	−0.045***	−0.018**	−0.018**	−0.018**	−0.017**	−0.018**	−0.018***	−0.412***
	(0.011)	(0.014)	(0.007)	(0.007)	(0.007)	(0.007)	(0.007)	(0.002)	(0.156)
Control mean	0.093	0.093	0.058	0.058	0.058	0.058	0.058	0.058	0.058
Num. obs.	127,314,386	127,144,992	11,423,056	11,423,056	11,423,056	11,423,056	11,423,056	1,142,306	11,423,056
Sample	Unmatched	Unmatched	Full matched	Full matched	Full matched	Full matched	Full matched	10% subsample	Full matched
Estimator	OLS	OLS	OLS	OLS	OLS	OLS	OLS	OLS	Frac. logit
Country FE	No	Yes	No	Yes	Yes	Yes	Yes	Yes	Yes
Biome FE	No	Yes	No	No	Yes	Yes	No	Yes	No
PA FE	No	No	No	No	No	No	Yes	No	No
Matching covariates	No	No	No	No	No	Yes	No	No	No
SE type	Country	Country	Country	Country	Country	Country	Country	Conley (100 km)	Country

Note: For all models the dependent variable is the threat composite index. Model (1) uses the full unmatched sample without fixed effects (FE) or controls. Model (2) adds country and biome fixed effects to the unmatched sample. Models (3)–(7) use the matched sample. Model (3) is an OLS regression without fixed effects or control variables. Model (4) adds country fixed effects. Model (5) adds biome fixed effects. Model (6) adds the eight matching covariates as controls (elevation, population density, precipitation, slope, temperature, travel time, crop suitability, tree cover). Model (7) replaces biome fixed effects with protected area fixed effects. Model (8) uses a random 10% subsample of the matched data with country and biome fixed effects and Conley spatial standard errors (SE). Model (9) uses a fractional logit specification (log-odds) with country fixed effects on the matched sample. The identical point estimates across columns (3)–(5) reflect the 1:1 matching design within country–biome strata, since treatment assignment is perfectly balanced (50% treated, 50% control) within each country, country and biome fixed effects are orthogonal to the treatment indicator and leave the coefficient unchanged. * $p < 0.1$, ** $p < 0.05$, *** $p < 0.01$. Standard errors in parentheses.

Table C.3: Sensitivity test results

Variable	Norm. mean diff.	Risk ratio	E-value	Γ (α=0.05)	Γ (α=0.01)
Built area [sqm]	−0.033	0.970	1.208	>3.0	>3.0
Cropland [%]	−0.082	0.928	1.365	>3.0	>3.0
Forest plantation [%]	0.001	1.001	1.029	1.0	1.0
No. of cattle	−0.058	0.949	1.293	>3.0	>3.0
Oil & gas operation [%]	0.000	1.000	1.016	1.0	1.0
Mining operations [%]	−0.022	0.980	1.163	>3.0	>3.0
Renewable energy presence [%]	−0.006	0.995	1.078	>3.0	>3.0
Road presence [%]	−0.026	0.976	1.182	>3.0	>3.0
Power lines presence [%]	−0.039	0.965	1.231	>3.0	>3.0
Burned area presence [%]	−0.001	0.999	1.034	>3.0	>3.0
Surface water change [% change]	−0.021	0.981	1.159	>3.0	>3.0
Dams presence [%]	0.001	1.001	1.025	1.0	1.0
Light intensity	−0.043	0.961	1.244	>3.0	>3.0
Forest loss 2001-2020 [sqm]	−0.239	0.804	1.794	>3.0	>3.0
Any threat [%]	−0.102	0.911	1.425	>3.0	>3.0
Threat composite [0-1]	−0.141	0.880	1.531	>3.0	>3.0

Note: The normalized mean difference and converted to an approximate risk ratio. Higher E-values indicate greater robustness to unmeasured confounding variables. Γ reports the critical value of the Rosenbaum bounds sensitivity parameter at which the treatment effect first becomes non-significant at the indicated level. Higher Γ values indicate less sensitive results.

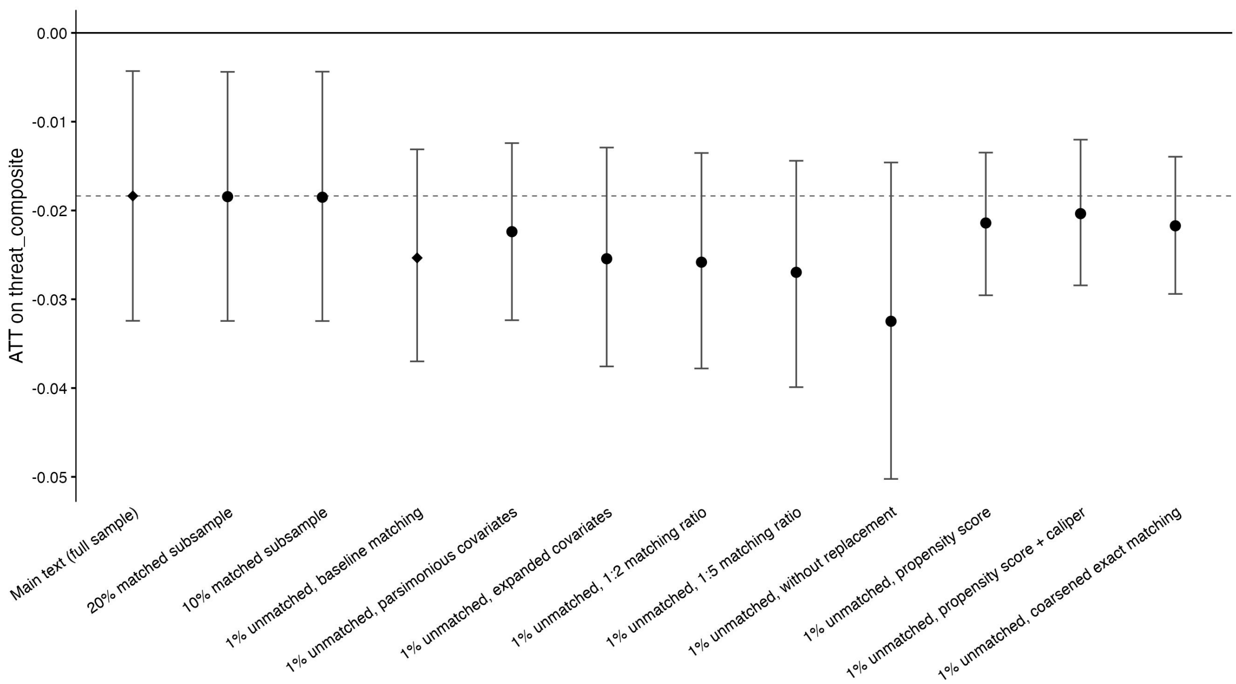

Figure C.5: **Robustness of the global ATT to random subsampling and alternative matching procedures.** Robustness of the main composite threat estimate (ATT) across alternative sample sizes and matching specifications. The leftmost point reproduces the main estimate with subsequent points re-estimating the model on random 20% and 10% subsamples (5 seeds each), and then applying alternative matching procedures to a stratified 1% subsample, including variations in covariate sets, matching ratios, replacement rules, propensity-score matching, and coarsened exact matching. Black points show the median estimate across seeds, grey whiskers show 95% confidence intervals, and the dashed line marks the main text estimate.

Table C.4: Robustness of the global ATT

Specification	ATT
Main text (full sample)	–0.018**
	(0.007)
20% matched subsample	–0.018**
	(0.007)
10% matched subsample	–0.019**
	(0.007)
1% unmatched, baseline matching	–0.025***
	(0.006)
1% unmatched, parsimonious covariates	–0.022***
	(0.005)
1% unmatched, expanded covariates (with climate quadratics)	–0.025***
	(0.006)
1% unmatched, 1:2 matching ratio	–0.026***
	(0.006)
1% unmatched, 1:5 matching ratio	–0.027***
	(0.006)
1% unmatched, without replacement	–0.032***
	(0.009)
1% unmatched, propensity score	–0.021***
	(0.004)
1% unmatched, propensity score (with 0.25 SD caliper)	–0.020***
	(0.004)
1% unmatched, coarsened exact matching	–0.022***
	(0.004)

Note: All estimates use country and biome fixed effects with country-clustered standard errors. For multi-seed rows, the point estimate and standard error are the median across 5 seeds; standard errors in parentheses. Significance stars based on median p-value across seeds: * p<0.1, ** p<0.05, *** p<0.01p. The first row reproduces the main text estimate. Subsequent rows re-estimate on random subsamples of the matched dataset, then apply the baseline matching procedure to a subsample of the unmatched data, varying one matching dimension at a time.

C.7 Supplementary Information: Heterogeneity

By biome. Figure B.1 plots the ATT on the composite threat index for each terrestrial biome. Table C.5 reports the area, PA area, and protection share of each biome; Table C.6 reports threat-specific ATTs by biome.

By country. Table C.7 reports threat-specific ATTs for the 106 countries with at least one estimable outcome among the 107 countries that meet the covariate-balance threshold (average $|\text{SMD}| \leq 0.10$).

By protected-area type (strict/multi-use, size). Figure B.3 reports threat-specific ATTs by IUCN management category (strict vs. multi-use) and PA size class. Figure C.6 aggregates the same breakdown to the composite threat index, and Table C.9 reports the underlying estimates and standard errors.

Matched-sample composition by PA designation year. Figure C.4 shows the distribution of the matched treated sample over PA designation years (2001–2020), counted as (a) distinct PAs and (b) treated 1 km^2 pixels.

Table C.5: Terrestrial area and protected area coverage by biome.

	Area (10^3 km^2)	PA area (10^3 km^2)	PA coverage (%)	Share of land (%)	Share of all PAs (%)
Trop. moist forests	18 315.7	4054.0	22.1	14.5	24.8
Trop. dry forests	2833.9	239.5	8.5	2.2	1.5
Trop. conif. forests	678.2	93.9	13.8	0.5	0.6
Temp. broadleaf forests	12 311.2	1377.7	11.2	9.8	8.4
Temp. conif. forests	3994.8	552.3	13.8	3.2	3.4
Boreal forests/taiga	14 973.7	1609.2	10.7	11.9	9.9
Trop. grasslands	19 217.2	2987.5	15.5	15.2	18.3
Temp. grasslands	9975.5	430.2	4.3	7.9	2.6
Flooded grasslands	906.5	246.7	27.2	0.7	1.5
Montane grasslands	5058.2	380.8	7.5	4.0	2.3
Tundra	7561.0	1166.9	15.4	6.0	7.1
Mediterranean	3071.1	450.9	14.7	2.4	2.8
Deserts & xeric	27 070.1	2707.5	10.0	21.4	16.6
Mangroves	262.4	36.0	13.7	0.2	0.2
Global	126 229.3	16 333.2	12.9	100.0	100.0

Note: PA coverage is the percentage of each biome under protection. Share of land and share of all PAs indicate each biome's contribution to the global totals.

Table C.6: Protected areas effect by biome

	Built area [sqm]	Cropland [%]	Forest planta-tion [%]	No. of cattle	Oil & gas operation [%]	Mining opera-tions [%]	Renewable energy presence [%]	Road presence [%]	Power lines presence [%]	Burned area presence [%]	Surface water change [% change]	Dams presence [%]	Light in-tensity	Forest loss 2001-2020 [sqm]	Any threat [%]	Threat compos-ite [0-1]
	(1)	(2)	(3)	(4)	(5)	(6)	(7)	(8)	(9)	(10)	(11)	(12)	(13)	(14)	(15)	(16)
Trop. moist forests	-129.1*	-0.100*	-0.367*	-238.6***	0.000	-0.031**	-0.000	-0.677**	-1.05***	-0.028	3.47*	0.002	-0.253	-0.074***	-0.158***	-0.035***
Trop. dry forests	-368.2	-3.32***	-0.501	-291.3***	NA	0.012	0.000	-4.47***	-1.96*	0.724	19.09*	0.022***	-0.397***	-0.046**	-0.045*	-0.027***
Trop. conif. forests	-224.0***	-0.420**	0.119**	-80.46	NA	-0.078***	-0.000	-1.68***	-0.148	0.015***	-32.00*	0.016*	0.199***	-0.002**	-0.015***	-0.004**
Temp. broadleaf forests	-1824.1***	-5.86***	3.57**	-225.0***	0.001	-0.091	-0.065	-2.75***	-2.91***	0.209	1.01	0.047***	-0.518***	-0.021	-0.051**	-0.029***
Temp. conif. forests	-587.8	-0.548**	-2.27	-76.06**	NA	-0.063**	-0.051	-0.030	-1.90***	-0.005	-2.01	0.019	-0.167	-0.012*	-0.017	-0.008***
Boreal forests/taiga	-36.15	-0.066	NA	-1.53**	NA	-0.083***	-0.003	-0.398	-0.470*	-0.043	-0.871***	-0.002	-0.117***	-0.018**	-0.020	-0.006
Trop. grasslands	-74.45	-1.14*	-0.078*	-110.8	-0.000*	-0.045**	-0.001	-0.266	-0.252	-0.273	-0.511	-0.013	0.275	-0.039***	-0.013	-0.007
Temp. grasslands	-452.4**	-10.56***	7.84	-54.00**	-0.005	-0.438**	-0.002	-1.95*	-1.28***	-0.317	4.67	-0.020	-0.282	0.004	-0.077***	-0.028***
Flooded grasslands	-116.1	-1.38	NA	188.6	0.004	0.003	NA	-5.65**	-0.311	0.266	-14.28	NA	-0.904	-0.010	-0.053	-0.008
Montane grasslands	105.3	1.24	-0.333	421.8	NA	-0.141	NA	-0.341	-0.129	0.484	-1.62	0.002	-0.259**	-0.002	-0.000	0.003
Tundra	-1.06	-0.001	NA	-5.82	NA	-0.017	-0.001	0.097	-0.124	-0.007	1.33***	-0.001	0.108	0.007***	0.000	-0.001
Mediterranean	-1721.4**	-9.90***	3.13	-59.88**	-0.001	-0.239*	-0.084	-2.55***	-2.10**	0.905	1.09	0.035	-0.747**	0.003	-0.016***	-0.018***
Deserts & xeric	-685.8	-0.444	-0.122	-25.94***	-0.000	-0.158*	-0.003	-0.475	-0.482	-0.027*	0.496	-0.008	-0.746	-0.028**	-0.054	-0.010
Mangroves	-927.0	-1.41	-3.68	43.25	NA	NA	NA	-7.40	0.347	0.018	12.59	-0.037	-0.462	-0.046	0.109	-0.013

Note: Average treatment effect on the treated (ATT) from biome OLS regressions with country fixed effects and country-clustered standard errors. Biomes with a single country use heteroskedasticity-robust standard errors without fixed effects. NA indicates the threat is not observed in that biome or the sample is too small for estimation. */ **/ *** denote $p < 0.1/0.05/0.01$, respectively.

Table C.7: Protected areas effect by country

	Built area [sqm]	Cropland [%]	Forest plantation [%]	No. of cattle	Oil & gas operation [%]	Mining operations [%]	Renewable energy presence [%]	Road presence [%]	Power lines presence [%]	Burned area presence [%]	Surface water change [% change]	Dams presence [%]	Light intensity	Forest loss 2001-2020 [sqm]	Any threat [%]	Threat composite [0-1]
	(1)	(2)	(3)	(4)	(5)	(6)	(7)	(8)	(9)	(10)	(11)	(12)	(13)	(14)	(15)	(16)
Algeria	-140.5	-4.38***	NA	-23.71***	NA	-0.017**	0.003	1.14***	-0.933***	0.003	-38.97***	-0.003	-0.919***	0.000	-0.070***	-0.016***
Angola	48.98***	-0.039***	NA	-0.585*	NA	NA	NA	-0.894***	0.247***	0.396***	0.903	NA	0.223***	-0.022***	0.010***	0.001***
Argentina	293.6***	-1.62***	NA	-228.7***	NA	-0.034***	NA	-2.63***	-0.371***	-0.015	1.57**	0.000	0.084**	-0.023***	-0.015***	-0.013***
Australia	-93.80***	-1.60***	NA	-74.77***	-0.000	-0.258***	-0.002***	-1.21***	-0.168***	0.207***	-0.401	0.001*	0.356***	-0.058***	0.010***	-0.003***
Austria	-2204.0***	-2.70***	-2.32***	-69.54***	NA	NA	-0.325***	-0.146	-3.78***	NA	NA	-0.179***	-1.01***	0.003*	-0.014**	-0.015***
Azerbaijan	-2030.0***	-10.21***	NA	-633.3***	NA	NA	NA	0.508	3.56*	NA	NA	NA	0.936***	0.004**	0.014	-0.037***
Bangladesh	-2832.8***	-2.91**	NA	649.6*	NA	NA	NA	-29.36***	-3.88**	NA	NA	NA	0.468*	-0.020	0.017***	-0.049***
Belarus	-2694.6***	-17.66***	0.238	17.92*	NA	-0.026	NA	-5.14***	-7.07***	NA	31.31***	NA	-0.219***	-0.014***	-0.046***	-0.060***
Benin	-8876.9*	-40.05***	NA	-1153.6***	NA	NA	NA	-43.59***	-5.13	NA	NA	NA	-2.67***	NA	NA	-0.169***
Bolivia	1277.7***	-0.834***	NA	47.12***	NA	NA	NA	-1.35***	-0.277**	0.025*	-4.44	NA	-0.046	-0.012***	0.038***	-0.004***
Bosnia and Herzegovina	62.36	-0.614	-1.94***	-100.5***	NA	NA	NA	12.29***	0.776	0.129	NA	-0.129	0.276	-0.007***	0.031***	0.005
Brazil	-65.94***	-0.303***	-0.208***	-377.0***	NA	-0.054***	-0.003***	-0.235***	-1.54***	0.012***	5.75***	-0.000	-0.410***	-0.097***	-0.201***	-0.047***
Bulgaria	-1549.7***	-5.06***	3.46***	-24.83***	NA	-0.412***	0.028*	-1.34***	-4.26***	0.012**	-1.41	0.034	-0.437***	-0.006***	-0.028***	-0.022***
Cameroon	-2427.5***	-1.37***	-0.013	-53.76***	NA	NA	NA	-11.04***	-6.54***	0.676***	19.73***	0.004	0.534***	-0.008***	-0.161***	-0.020***
Canada	-39.36***	-0.932***	NA	-4.24***	-0.000	-0.074***	-0.001**	-0.294***	-0.340***	-0.000	-0.105	-0.007***	-0.186***	-0.025***	-0.033***	-0.004***
Chad	-145.1**	-3.36***	NA	-471.2***	NA	NA	NA	0.185	-0.104***	0.370	NA	NA	-0.061	NA	-0.002***	-0.029***
Chile	-14.82***	-0.015***	NA	-36.32***	NA	-0.058***	-0.015**	-0.240**	-0.150***	0.004	-10.11**	NA	-0.063***	0.002*	-0.013***	-0.001**
China	-294.0***	-5.52***	NA	-48.68**	NA	NA	NA	-2.09	-3.77***	NA	38.60**	NA	-0.498***	0.010	-0.067	-0.022***
Colombia	-1497.2***	-0.172***	-0.443***	-223.2***	NA	-0.008	NA	-4.75***	-1.42***	-0.022	-2.92	0.018***	-0.378***	-0.011***	-0.052***	-0.019***
Côte d'Ivoire	-2131.5*	0.215	-0.491	29.97***	NA	NA	NA	-7.75***	3.24***	0.393**	NA	NA	0.204	-0.000	-0.008***	-0.040***
Croatia	-1778.5***	-2.88***	0.869***	-34.73***	NA	-0.032	0.065***	-0.227	-2.31***	NA	88.38***	0.049**	-0.368***	0.000	-0.021***	-0.012***
Democratic Republic of the Congo	229.7***	0.171***	-0.043***	23.89***	NA	NA	NA	0.418***	0.895***	-2.04***	1.96**	NA	0.590***	0.006***	-0.030***	0.003***
Djibouti	-440.1*	NA	NA	-100.0***	NA	NA	NA	2.96	-7.39***	NA	NA	NA	-0.453***	NA	NA	-0.004
Ecuador	-585.3***	-0.085***	NA	-787.0***	0.005	NA	NA	-8.39***	-2.23***	NA	15.45**	0.016*	0.258***	-0.018***	-0.019***	-0.026***
El Salvador	1119.7	4.43***	NA	-2222.6***	NA	NA	NA	-20.52***	-22.68***	NA	NA	0.432**	-0.843***	-0.007*	-0.003*	-0.087***
Estonia	-2143.3***	-14.39***	NA	-114.5***	NA	-5.67***	-0.203**	-9.05***	-9.42***	NA	-0.451	NA	-3.58***	-0.035***	-0.192***	-0.073***
Ethiopia	-2.37	1.33***	NA	579.1***	NA	NA	0.000	-0.035	-0.598***	0.301***	7.23	-0.005	-0.018	0.013*	0.055***	0.006***
Finland	-654.2***	-2.04***	NA	-13.46***	NA	-0.079**	-0.023	-4.51***	-2.87***	NA	-0.107	-0.011	-0.471***	-0.077***	-0.179***	-0.034***

Continued on next page

Table C.7 continued

	Built area [sqm]	Cropland [%]	Forest plantation [%]	No. of cattle	Oil & gas operation [%]	Mining operations [%]	Renewable energy presence [%]	Road presence [%]	Power lines presence [%]	Burned area presence [%]	Surface water change [% change]	Dams presence [%]	Light intensity	Forest loss 2001-2020 [sqm]	Any threat [%]	Threat composite [0-1]
	(1)	(2)	(3)	(4)	(5)	(6)	(7)	(8)	(9)	(10)	(11)	(12)	(13)	(14)	(15)	(16)
France	-3794.0***	-6.96***	8.66***	-268.3***	NA	-0.058***	-0.295***	-5.27***	-2.50***	0.003	15.50*	0.066***	-0.618***	0.003***	0.002***	-0.026***
Gabon	10.50	-0.003***	0.062***	-0.439***	NA	-0.005	NA	-0.020	0.316***	0.040*	0.560	0.002	-0.108***	0.000	-0.032***	-0.000
Gambia	167.2	0.083	NA	494.0	NA	NA	NA	0.000	NA	NA	NA	NA	-0.917	NA	-0.083	0.002
Guatemala	-1553.7***	-0.239***	0.206	234.4**	NA	0.083	NA	-9.91***	-4.62***	0.041	NA	NA	-1.67***	-0.070***	-0.073***	-0.037***
Guinea	641.1***	-0.296***	NA	28.38***	NA	0.020*	NA	-5.90***	2.53***	-2.69***	-17.64	NA	0.158***	NA	-0.001***	-0.004***
Guyana	-11.94***	-0.006***	NA	-0.912***	NA	-0.030**	NA	-1.21***	-0.105***	-0.015	15.00	NA	-0.155***	-0.003***	0.004	-0.004***
Honduras	262.8	0.055***	-1.51***	-621.8***	NA	NA	NA	1.07	1.07	NA	NA	NA	0.187	0.005	-0.008***	-0.013***
Iceland	-1226.4***	-0.310***	NA	5.41**	NA	NA	NA	-8.21***	-5.83***	NA	15.33	NA	-2.94***	NA	-0.146***	-0.042***
Indonesia	-274.0***	-4.46***	NA	-86.95***	NA	NA	NA	-9.04***	-0.107**	NA	25.83**	NA	-2.77***	-0.057***	-0.138***	-0.051***
Iran	-113.0	-0.410***	NA	-21.23***	NA	-0.054***	NA	0.936***	-0.285*	-0.032*	7.10	NA	-0.006	NA	0.003	-0.001
Iraq	-2035.2***	-12.62***	NA	2.66	-0.000	NA	NA	-25.67***	-8.38***	0.232	-49.48***	NA	-13.15***	-0.016***	-0.027***	-0.141***
Ireland	-2954.0***	-2.65***	20.83***	-2256.5***	NA	0.035	-0.106	-10.61***	-5.45***	NA	-5.64	NA	-1.40***	0.059***	-0.006***	-0.057***
Italy	-3834.4***	-3.00***	0.511**	-158.0***	NA	-0.019	-0.074**	-6.19***	-5.26***	0.004	2.60	0.137***	-1.36***	-0.000	-0.012***	-0.030***
Japan	-1446.7***	-1.10***	NA	-68.76***	NA	-0.091***	0.046**	3.15***	-2.69***	NA	-2.46	0.207***	0.096	-0.008***	-0.055***	-0.009***
Jordan	-311.6**	0.323***	NA	-2.31**	NA	-1.58***	NA	2.47***	-0.259	NA	NA	NA	-0.322***	NA	0.060***	0.001
Kazakhstan	-112.7***	-2.86***	NA	-4.54***	NA	-0.129***	-0.000	-0.502***	-0.367***	-0.287***	-5.66***	-0.000	-0.408***	0.000	-0.063***	-0.014***
Kenya	-818.5***	-2.30***	0.018	1887.2***	NA	NA	NA	-0.212	-0.083	NA	-36.82*	NA	-0.586***	-0.015	0.047***	0.053***
Laos	-118.2***	-1.56***	NA	-107.3***	NA	-0.013	NA	-1.94***	-2.16***	0.110***	4.50**	0.006	-0.532***	-0.087***	-0.164***	-0.053***
Latvia	-1442.3***	-9.76***	NA	-155.6***	NA	NA	NA	-4.61***	-9.62***	NA	-17.66***	NA	-0.841***	-0.058***	-0.133***	-0.061***
Lebanon	-4135.3**	4.43***	NA	-107.1***	NA	NA	NA	-11.30***	-3.04	NA	NA	NA	-4.11***	0.017	NA	-0.043***
Liberia	-185.5***	NA	-0.185	22.93***	NA	-0.463**	NA	-15.17***	-0.093	0.185	NA	NA	0.245***	-0.046***	-0.219***	-0.066***
Libya	25.64	NA	NA	-0.000*	NA	NA	NA	0.000	NA	NA	NA	NA	NA	NA	0.007	0.000
Lithuania	-2401.8***	-22.77***	0.053	-135.0***	NA	NA	0.053	-13.68***	-9.42***	NA	-1.89	-0.053	-0.501***	0.058***	-0.006***	-0.083***
Madagascar	-141.1***	1.25***	NA	-205.1***	NA	0.024***	NA	-1.60***	0.006	0.032	-5.29**	0.012**	-0.323***	-0.091***	-0.067***	-0.010***
Malawi	-2707.7***	2.07*	NA	594.0***	NA	NA	NA	-7.55***	-8.58***	0.458**	7.81*	NA	-0.650***	NA	NA	0.006
Malaysia	-341.7***	-0.016***	-9.20***	-47.64***	NA	-0.012	NA	-0.309**	-0.535***	NA	1.10	0.012*	-0.796***	-0.146***	-0.182***	-0.084***
Mali	-191.8***	-2.44***	NA	793.3***	NA	NA	NA	-4.19***	-0.234***	0.045	-10.70***	NA	0.083***	NA	0.012***	0.022***
México	-383.7***	-1.91***	-0.111***	-67.79***	0.001	-0.008	0.001	-1.47***	-0.760***	0.015*	10.28***	-0.068***	0.045*	-0.016***	-0.007***	-0.007***
Mongolia	-21.46***	-0.326***	NA	-41.11***	NA	-0.001	NA	-1.14***	-0.769***	NA	-23.74	NA	-0.066***	0.092***	-0.027***	-0.002***
Morocco	-174.7**	0.903***	NA	-0.647	NA	NA	NA	-0.268	-2.27***	NA	-7.19	0.041	0.344***	0.004	0.150***	0.003*
Mozambique	-413.9***	-1.17***	NA	-95.80***	NA	NA	NA	-2.55***	0.117	-0.064	-51.50***	0.002	-0.590***	-0.023**	-0.098***	-0.008***
Myanmar	47.41***	-0.048	0.101*	-1.96	NA	NA	NA	0.432**	0.675***	-0.018**	15.38*	NA	-0.008	-0.024***	-0.038***	-0.008***

Continued on next page

Table C.7 continued

	Built area [sqm]	Cropland [%]	Forest plantation [%]	No. of cattle	Oil & gas operation [%]	Mining operations [%]	Renewable energy presence [%]	Road presence [%]	Power lines presence [%]	Burned area presence [%]	Surface water change [% change]	Dams presence [%]	Light intensity	Forest loss 2001-2020 [sqm]	Any threat [%]	Threat composite [0-1]
	(1)	(2)	(3)	(4)	(5)	(6)	(7)	(8)	(9)	(10)	(11)	(12)	(13)	(14)	(15)	(16)
Namibia	-3358.3***	-0.372***	NA	-93.64***	NA	0.040***	0.000	0.916***	0.489***	0.012	-7.40***	0.002	-1.13***	NA	-0.107***	-0.007***
Nepal	1171.7***	-1.15***	0.015	-475.9***	NA	NA	NA	1.79***	1.12***	NA	-39.33***	0.030	-0.283***	0.000	-0.023***	-0.011***
Niger	18.57	0.575***	NA	174.0***	NA	NA	NA	-0.362***	0.115***	NA	1.73	0.002*	-0.229***	NA	-0.033***	0.009***
North Korea	-566.1	-4.67	NA	508.0***	NA	NA	NA	-33.33*	-11.11	NA	NA	NA	9.78***	0.003	0.222	-0.067*
North Macedonia	-3483.9***	-2.92***	NA	-98.25***	NA	NA	NA	-2.30	-12.90***	NA	NA	0.461	-1.34***	-0.020***	-0.028*	-0.033***
Norway	-208.5***	-0.231***	NA	-22.89***	NA	NA	-0.083*	-4.22***	-5.70***	NA	-5.47	-0.033	-1.41***	-0.030***	-0.148***	-0.023***
Pakistan	-35.02	-0.866***	0.034	-206.3***	NA	-0.068	NA	0.851	1.67***	NA	NA	NA	-0.400***	-0.000	-0.063***	-0.007***
Panama	-123.4*	-0.171***	NA	4.36	NA	1.14***	0.031	-1.69***	-0.246	NA	-19.57	NA	-0.069	-0.019***	-0.065***	-0.009***
Paraguay	-423.3**	-2.59***	NA	-557.1***	NA	NA	NA	-1.27***	-2.24***	0.179**	12.87**	NA	-0.343***	-0.061***	0.024***	-0.049***
Peru	-70.29***	-0.023***	-0.017***	-45.97***	NA	-0.057***	NA	-0.118**	0.021	NA	-1.24	-0.001	-0.343***	-0.028***	-0.096***	-0.012***
Philippines	49.11	-0.908***	-6.48***	-24.83***	NA	0.026	0.026	-0.603**	-1.47***	0.077**	-2.13	0.006	-0.243***	-0.006***	-0.036***	-0.010***
Poland	-3523.8***	-25.24***	-0.065***	-337.7***	0.007	0.337***	-0.058***	-4.42***	-6.07***	NA	25.30***	0.007	-1.31***	0.029***	-0.004***	-0.076***
Portugal	-490.5**	-0.934***	NA	-178.8***	NA	0.012	0.331***	5.44***	1.58**	-0.165***	-17.22	0.071	-0.244**	-0.043***	NA	-0.004**
Republic of the Congo	-61.30**	-0.088***	0.004	-1.48***	NA	NA	NA	0.304***	0.319***	-0.052	26.17	NA	1.26***	-0.001*	0.007***	0.004***
Romania	-3314.0***	-10.16***	4.64***	-80.55***	NA	-0.018	0.006	-4.66***	-3.73***	0.066***	55.18***	0.078***	-1.22***	0.003***	-0.028***	-0.041***
Russia	-100.0***	-1.09***	NA	-3.73***	NA	-0.134***	0.000	0.047	-0.536***	-0.052***	-0.029	-0.001	0.070***	-0.011***	-0.012***	-0.008***
Rwanda	-13374.9***	-18.37***	-13.08***	-668.8***	NA	NA	NA	-41.12***	-0.935	0.935	NA	NA	-0.028	-0.128***	NA	-0.156***
Saudi Arabia	-1047.3***	-1.39***	NA	-8.11***	NA	0.001	NA	0.017	-3.61***	NA	NA	NA	-4.83***	NA	-0.299***	-0.058***
Senegal	-168.8*	0.157**	NA	-106.9***	NA	NA	NA	-3.81***	-0.166	0.746*	NA	NA	-0.143	NA	0.013***	-0.008***
Serbia	-3031.1***	-9.29***	5.05***	-95.29***	NA	-0.241	NA	3.01*	-4.21**	NA	15.58	0.120	-0.048	0.019***	0.010**	-0.024***
South Africa	-647.6***	-0.919***	-0.950***	18.12***	NA	-0.392***	NA	0.977***	-1.67***	0.039	9.53	-0.019	-0.777***	-0.092***	0.060***	-0.005***
South Korea	-2958.7***	-3.21***	-4.39***	-670.5***	NA	0.067	0.033	2.65***	-3.96***	NA	3.19	0.145***	0.239	-0.021***	-0.014***	-0.024***
South Sudan	183.0***	0.021***	NA	-609.7***	NA	NA	NA	0.949***	-0.438***	-0.903***	24.84***	NA	0.529***	-0.004	-0.128***	-0.029***
Spain	-2366.1***	-6.78***	NA	-47.86***	NA	-0.061***	-0.210***	-2.92***	-3.63***	NA	9.34	0.080***	-1.36***	-0.008***	-0.012***	-0.027***
Sudan	7.66	NA	NA	-13.02	NA	NA	NA	7.24***	NA	NA	NA	NA	0.039	NA	0.151***	0.003**
Swaziland	-2022.7	-1.86	NA	41.45	NA	NA	NA	-5.56	-13.89**	NA	NA	5.56	0.806**	NA	NA	-0.023*
Sweden	-881.3***	-4.45***	NA	-51.93***	NA	0.041	-0.071**	-8.20***	-4.28***	NA	1.05	-0.031*	-0.256**	-0.031***	-0.172***	-0.035***
Switzerland	-10145.5***	-1.73**	NA	-132.1	NA	NA	NA	-8.58***	-11.03***	NA	5.96*	NA	1.16*	-0.004	0.042	-0.034***
Taiwan	-5941.3***	-0.126	4.85	-22.33	NA	NA	NA	-19.42***	-11.65**	NA	NA	NA	-4.61**	-0.006	-0.029	-0.073***
Tajikistan	-2027.3**	-3.55***	NA	-390.2***	NA	NA	NA	0.000	-7.58*	NA	NA	NA	-2.55***	NA	0.106**	-0.041***

Continued on next page

Table C.7 continued

	Built area [sqm]	Cropland [%]	Forest plan-tation [%]	No. of cattle	Oil & gas operation [%]	Mining oper-ations [%]	Renewable energy presence [%]	Road presence [%]	Power lines presence [%]	Burned area presence [%]	Surface water change [% change]	Dams presence [%]	Light in-tensity	Forest loss 2001-2020 [sqm]	Any threat [%]	Threat com-posite [0-1]
	(1)	(2)	(3)	(4)	(5)	(6)	(7)	(8)	(9)	(10)	(11)	(12)	(13)	(14)	(15)	(16)
Tanzania	-1981.8***	-8.86***	NA	-595.6***	NA	-0.006	NA	-0.080	-0.725***	1.28***	2.53	NA	0.459***	-0.076***	-0.081***	-0.057***
Togo	-2140.9***	-6.56***	NA	9.52	NA	NA	NA	1.04	-8.33***	4.86***	NA	NA	0.562**	NA	0.017*	-0.028***
Tunisia	-1922.5***	-1.89***	NA	-19.29***	NA	0.024	NA	-1.12**	-0.923**	NA	24.09	0.000	-1.85***	-0.116***	-0.136***	-0.020***
Turkey	200.7	-10.71**	NA	-112.2	NA	NA	NA	-1.43	1.43	NA	NA	NA	-0.914	-0.055	0.086**	-0.031*
Uganda	-1159.4***	-4.84***	NA	3352.7***	NA	NA	NA	1.04**	-1.21***	-6.36***	20.26**	NA	-1.97***	-0.078***	-0.054***	-0.013***
Ukraine	-2566.3***	-14.30***	0.073	-22.61***	NA	-0.257*	NA	-4.22***	-7.59***	0.037	30.71	0.110*	0.728***	-0.010***	-0.026***	-0.072***
United Arab Emirates	-1006.1***	0.005	NA	-10.45***	NA	0.023*	0.031**	-1.65***	-0.416	NA	-10.40	NA	-3.58***	NA	-0.162***	-0.043***
United Kingdom	-2371.5***	-3.19***	0.374	-465.8***	NA	-0.072*	-1.38***	-0.648	-2.26***	NA	12.60	0.072**	-0.509***	0.009*	-0.015***	-0.021***
United States	-678.4***	-2.58***	-1.90***	-95.63***	-0.012**	-0.193***	-0.108***	-1.44***	-2.94***	0.095***	-0.769	0.015	-0.505***	-0.014***	-0.045***	-0.013***
Uruguay	10.69	-0.459	-1.29	-426.7***	NA	NA	NA	-3.19*	-0.603	NA	-52.35***	NA	-0.241*	-0.045***	0.003**	-0.024***
Uzbekistan	-716.2***	-1.35***	NA	-98.01***	NA	NA	NA	0.480*	-1.28***	NA	13.45*	NA	-1.40***	0.017*	-0.080***	-0.013***
Venezuela	-94.52	0.006	NA	-940.1***	NA	NA	NA	-1.73***	-2.56***	0.415*	67.43***	NA	-2.15***	-0.055***	-0.057***	-0.052***
Vietnam	-883.6***	-2.22***	-3.19***	-99.15***	NA	0.006	0.006	-3.69***	-0.863***	1.87***	17.82***	-0.000	-0.607***	-0.070***	-0.154***	-0.035***
Yemen	232.7	2.81***	NA	374.9***	NA	NA	NA	5.05**	2.45**	NA	NA	NA	0.756***	NA	0.052**	0.028***
Zambia	268.0***	0.812***	NA	8.60***	NA	NA	NA	-1.62***	0.015	-1.24***	NA	NA	-0.326***	NA	0.022**	0.003***
Zimbabwe	9.83	-3.02***	NA	-155.6***	NA	-0.010	NA	-0.481**	-0.000	0.005	-12.32	-0.289***	0.013	-0.042	-0.031***	-0.012***

Note: Average treatment effect on the treated (ATT) from within-country OLS regressions with biome fixed effects and heteroskedasticity-robust standard errors. Results are shown for 106 countries with at least one estimable outcome among the 107 countries meeting the covariate balance threshold (average $|SMD| \leq 0.10$). NA indicates the threat is not observed in that country or the sample is too small for estimation. */ **/ *** denote $p < 0.1/0.05/0.01$, respectively.

Table C.8: Distribution of protected areas by management category and size class

	N pixels (10^3 km^2)	Share (%)
IUCN management class		
Strict (Ia–IV)	2352.5	38.0
Multi-use (V–VI)	2158.0	34.9
Not Reported	1678.0	27.1
Size class		
Class 1 ($<$10 km^2)	56.9	0.9
Class 2 (10–500 km^2)	739.9	12.0
Class 3 (500–2000 km^2)	823.3	13.3
Class 4 ($>$2000 km^2)	4568.3	73.8

Note: Reports the protected-area pixel composition by IUCN management class and size class for the full protected-area sample. Based on the full sample of protected area pixels (no country exclusions). Shares computed within each group (IUCN management classes sum to 100%; size classes sum to 100%).

Table C.9: Threat differences based on protected area characteristics

	IUCN class			Size class			
	Strict (Ia-IV)	Multi-use (V-VI)	Not Reported	Class 1 (<10 km^2)	Class 2 (10-500 km^2)	Class 3 (500-2000 km^2)	Class 4 (>2000 km^2)
Built area [sqm]	−167.582***	−222.073**	−1 069.900**	−3 268.930***	−1 407.820***	−446.253***	−247.792
	(48.263)	(101.011)	(505.079)	(645.840)	(387.836)	(117.235)	(174.712)
	[584.669]	[654.250]	[2223.656]	[9636.402]	[3624.401]	[1609.680]	[478.270]
Cropland [%]	−0.956**	−1.070***	−2.274**	−4.531***	−4.093***	−2.980***	−0.613***
	(0.448)	(0.311)	(0.892)	(0.942)	(0.579)	(0.713)	(0.194)
	[2.344]	[1.905]	[6.015]	[13.697]	[10.471]	[6.837]	[1.315]
Forest plantation [%]	−0.537*	0.017	0.365	−0.630	−0.524	0.040	0.101
	(0.278)	(0.406)	(0.295)	(1.223)	(0.658)	(0.429)	(0.227)
	[0.949]	[2.413]	[1.942]	[7.831]	[7.807]	[3.284]	[0.544]
No. of cattle	−106.092	−104.778**	−123.191	−85.951***	−151.516***	−191.581***	−89.909
	(82.606)	(50.326)	(76.209)	(28.953)	(28.746)	(43.929)	(79.011)
	[421.838]	[481.620]	[717.199]	[903.941]	[939.801]	[812.923]	[404.246]
Oil & gas operation [%]	−0.000	−0.000	0.000	−0.005	−0.001	0.000**	0.000
	(0.000)	(0.000)	(0.000)	(0.004)	(0.002)	(0.000)	(0.000)
	[0.000]	[0.001]	[0.000]	[0.005]	[0.005]	[0.000]	[0.000]
Mining operations [%]	−0.077***	−0.128	−0.050*	−0.062	−0.151***	−0.087**	−0.080**
	(0.019)	(0.084)	(0.028)	(0.049)	(0.037)	(0.042)	(0.039)
	[0.085]	[0.194]	[0.095]	[0.268]	[0.204]	[0.137]	[0.113]
Renewable energy presence [%]	−0.004**	−0.009	−0.020	−0.029	−0.043**	−0.023*	−0.002
	(0.002)	(0.006)	(0.016)	(0.031)	(0.021)	(0.013)	(0.002)
	[0.007]	[0.016]	[0.046]	[0.095]	[0.079]	[0.053]	[0.003]
Road presence [%]	−0.963***	−0.687***	−0.968*	−3.044***	−2.270***	−1.376***	−0.552***
	(0.240)	(0.229)	(0.498)	(0.890)	(0.461)	(0.409)	(0.182)
	[4.537]	[5.390]	[9.455]	[26.634]	[17.418]	[10.735]	[3.479]
Power lines presence [%]	−0.732***	−0.800**	−1.207***	−3.425***	−2.326***	−1.093***	−0.609*
	(0.253)	(0.353)	(0.336)	(0.669)	(0.407)	(0.261)	(0.324)
	[2.082]	[2.439]	[5.185]	[16.105]	[9.702]	[5.449]	[1.496]
Burned area presence [%]	0.021	−0.014	−0.051	0.017	0.014	0.181**	−0.045
	(0.105)	(0.049)	(0.083)	(0.035)	(0.020)	(0.081)	(0.078)
	[0.464]	[0.349]	[0.256]	[0.250]	[0.290]	[0.560]	[0.348]
Surface water change [% change]	−0.758	2.163	−5.526	−1.282	−0.004	−6.312	−0.247
	(1.154)	(3.551)	(3.449)	(1.854)	(0.581)	(6.342)	(0.947)
	[-3.742]	[-18.848]	[-12.329]	[-8.302]	[-8.870]	[-3.629]	[-8.404]
Dams presence [%]	0.002	0.003	−0.003	0.090**	0.020*	−0.017	0.001
	(0.002)	(0.003)	(0.011)	(0.037)	(0.011)	(0.020)	(0.001)
	[0.004]	[0.005]	[0.024]	[0.056]	[0.032]	[0.039]	[0.001]
Light intensity	−0.312**	−0.262	−0.349*	0.259	−0.278	−0.509***	−0.276
	(0.120)	(0.354)	(0.177)	(0.241)	(0.217)	(0.135)	(0.210)
	[1.600]	[1.853]	[2.908]	[8.019]	[4.829]	[3.016]	[1.396]
Forest loss 2001-2020 [sqm]	−0.076**	−0.062***	−0.043**	−0.037***	−0.034***	−0.034**	−0.070***
	(0.030)	(0.014)	(0.020)	(0.009)	(0.008)	(0.014)	(0.021)
	[0.110]	[0.105]	[0.071]	[0.103]	[0.088]	[0.098]	[0.095]
Any threat [%]	−0.086**	−0.060	−0.068**	−0.034**	−0.040***	−0.058***	−0.079*
	(0.037)	(0.043)	(0.032)	(0.014)	(0.014)	(0.016)	(0.041)
	[0.476]	[0.405]	[0.607]	[0.904]	[0.787]	[0.669]	[0.405]
Threat composite [0-1]	−0.018**	−0.017**	−0.021***	−0.028***	−0.025***	−0.021***	−0.017*
	(0.009)	(0.008)	(0.007)	(0.004)	(0.003)	(0.004)	(0.009)
	[0.053]	[0.051]	[0.076]	[0.159]	[0.112]	[0.086]	[0.045]

Note: Average treatment effect on the treated (ATT). Standard errors clustered at the country level in parentheses, where */ **/ *** denote $p < 0.1/0.05/0.01$, respectively. Control means in brackets.

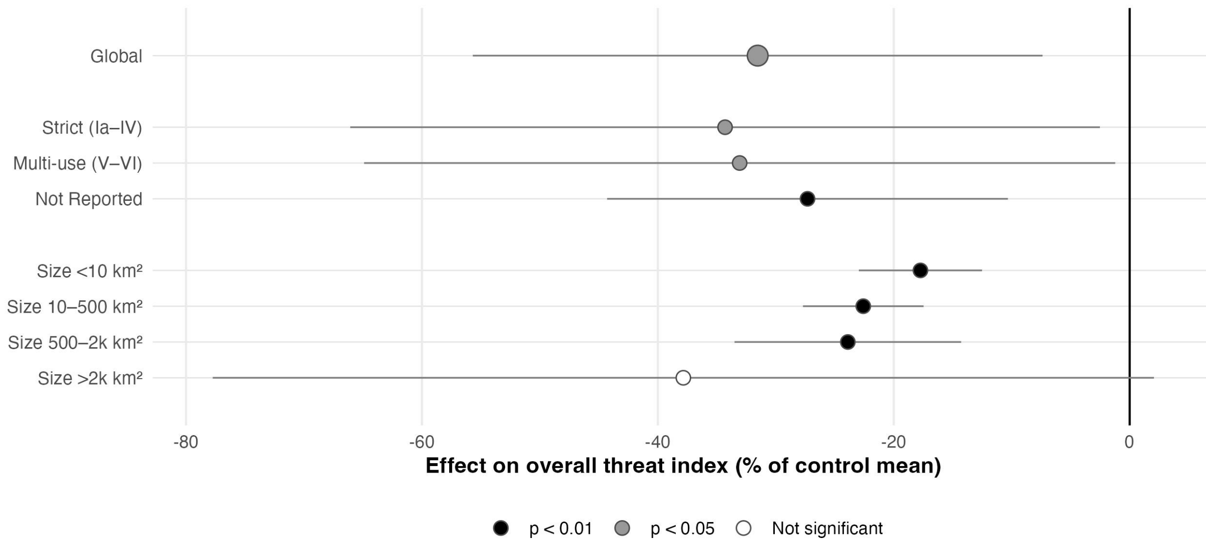

Figure C.6: **Effects by PA management category and size.** Treatment effects on the composite threat index, normalized as a percentage of the control mean, by IUCN management category, and PA size class. Point estimates with 95% confidence intervals. All regressions include country fixed effects with standard errors clustered at the country level.

C.8 Supplementary Information: Species- and taxon-level results

Taxon medians and biodiversity-weighted global ATT. Figure C.8 reports taxon-level medians of species-level percentage effects on the composite threat index alongside the global pixel-level ATT under five biodiversity-importance weighting schemes (equal weights, threatened-species richness, terminal branch length, evolutionary distinctiveness, EDGE2).

Conservation priorities tend to focus on the most threatened species first, with increasing attention also shifting to those that are evolutionarily distinct[56]. Estimated threat reductions may thereby be overvalued if the most effective PAs are located in low-biodiversity regions. To assess this, we combine our spatial database with the Evolutionarily Distinct and Globally Endangered (EDGE) approach[57], which ranks species by how much evolutionary history is at risk of extinction without conservation action. Re-estimating the composite threat index with weights based on threatened-species richness, terminal branch length, evolutionary distinctiveness, and EDGE2 scores, which combines these values into one metric[56], yields similar estimated reductions compared to the standard equal-weighted estimate (Fig. 5, Supplementary Fig. C.8). Furthermore, there is no trend observed between PAs located in more species-rich areas compared to species-poor areas (Extended Data Fig. B.4). Our assessed threat abatement in PAs, therefore, does not appear systematically stronger or weaker based on the underlying biodiversity at a site.

Distribution of species-level effects within taxa. The taxon medians in Figure 5A summarize the centre of each taxon's distribution but not its spread. Figure C.7 therefore plots the full distribution of species-level effects δ_s within each taxon on a common scale. The distributions are unimodal, centred below zero, and heavily overlapping, indicating that the similarity of the taxon medians reflects genuinely similar distributions rather than an artefact of the median. Reductions are the majority outcome in every taxon: the share of species with $\delta_s < 0$ is 86.6% for birds, 83.4% for mammals, 78.4% for amphibians, and 77.2% for reptiles, and 81.1% across all 3,310 species with estimable range-based regressions. Each distribution nevertheless has a right tail of species with higher composite threats inside protected pixels than in their matched controls, consistent with the species-level cases discussed in the main text.

Mammals. Figure C.9 reports per-species range coverage by protection status (panel A) and per-species effects on the composite threat index (panel B) for IUCN-listed threatened mammals.

Amphibians. Figure C.10 reports the same coverage and range-based effect summaries for IUCN-listed threatened amphibians.

Birds. Figure C.11 reports the same summaries for IUCN-listed threatened birds.

Reptiles. Figure C.12 reports the same summaries for IUCN-listed threatened reptiles.

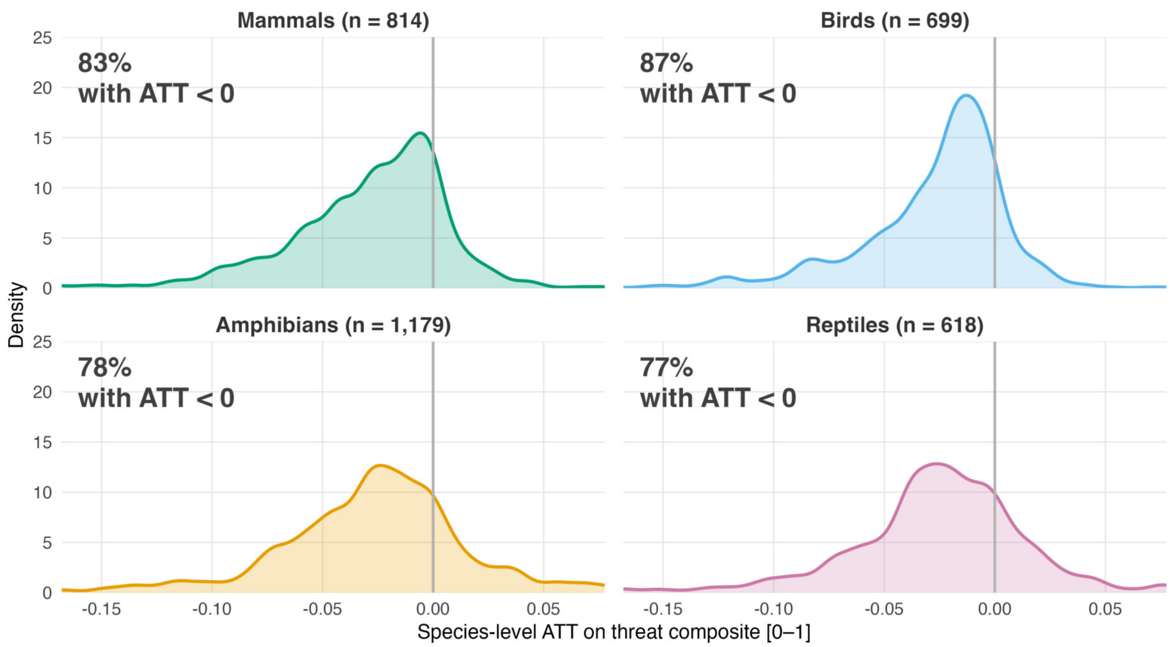

Figure C.7: **Distribution of species-level effects within taxa.** Kernel density of the species-range treatment effect δ_s on the composite threat index, shown separately for each vertebrate taxon on a common horizontal scale and a common bandwidth. Densities are estimated from every species with an estimable range-based regression ($n = 3{,}310$); only the displayed window is restricted. The vertical line marks zero, and each panel reports the number of contributing species and the share with $\delta_s < 0$, that is, with lower estimated composite threats inside protected pixels than in their matched controls.

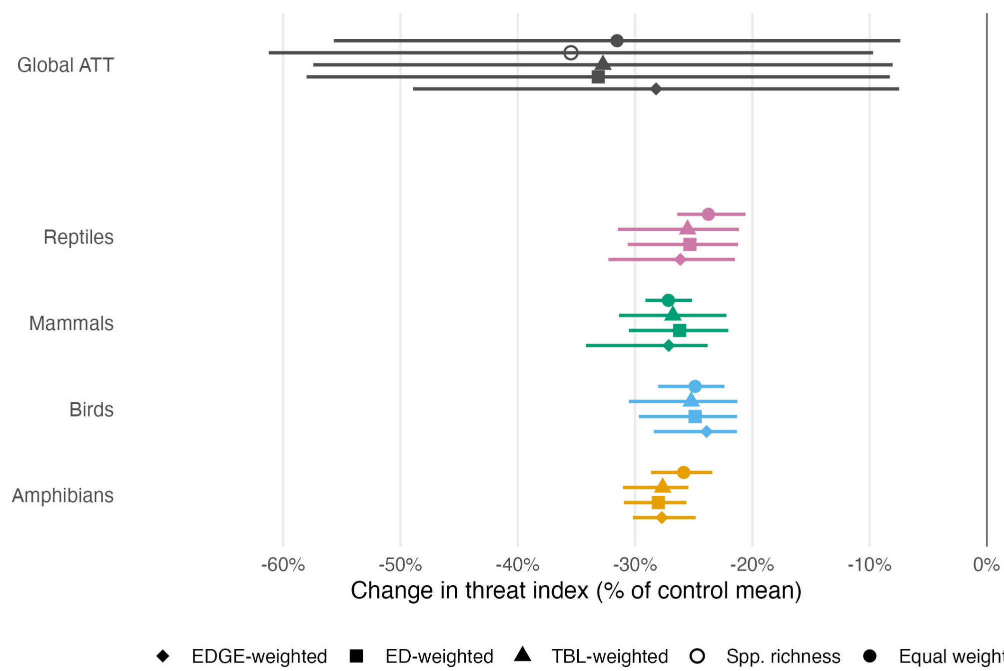

Figure C.8: **Varying species-level weightings.** Treatment effects are expressed as percentage changes in the composite threat index relative to matched controls. The Global ATT (black) shows pixel-level estimates under five biodiversity-weighting schemes: equal weights as the baseline (closed circle), threatened-species richness (open circle), terminal branch length (triangles), evolutionary distinctiveness (squares), and Evolutionarily Distinct and Globally Endangered (EDGE2) scores (diamonds). Lower rows show taxon-level median species effects under equal-species, terminal-branch-length, evolutionary-distinctiveness, and EDGE2 weighting, with 95% percentile-bootstrap confidence intervals from 2,000 within-taxon species resamples. Threatened-species-richness weighting is reported only for the Global ATT.

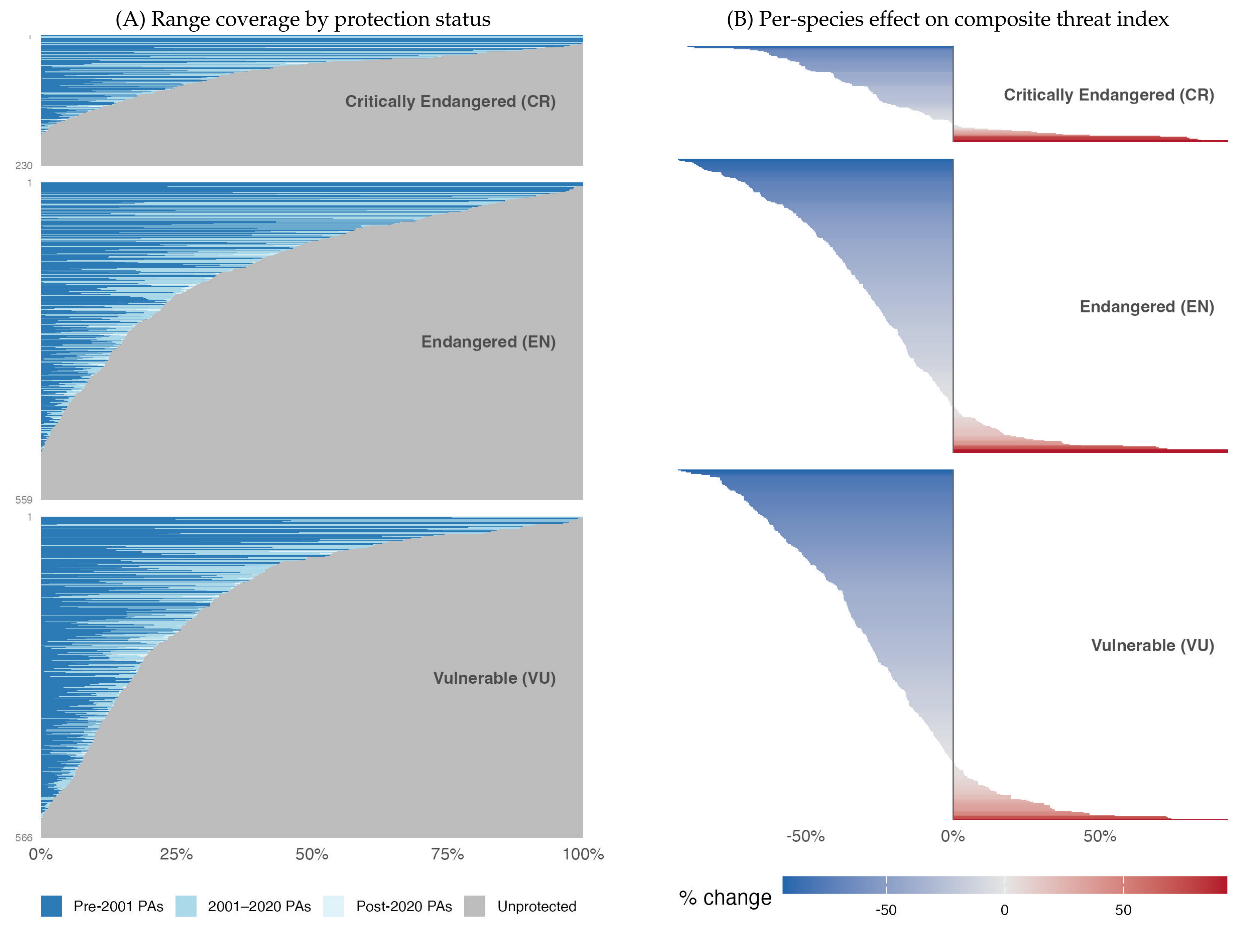

Figure C.9: **Species-level PA coverage and range-based effects — Mammals.** (a) Share of each threatened species' range covered by protected areas, with one bar per species. (b) Species-range FE estimate for the composite threat index, expressed as percentage change relative to matched controls, for species with an estimated coefficient. Blue indicates threat reduction, and red indicates threat increase. Values beyond the 1st and 99th percentiles are trimmed to the axis limits.

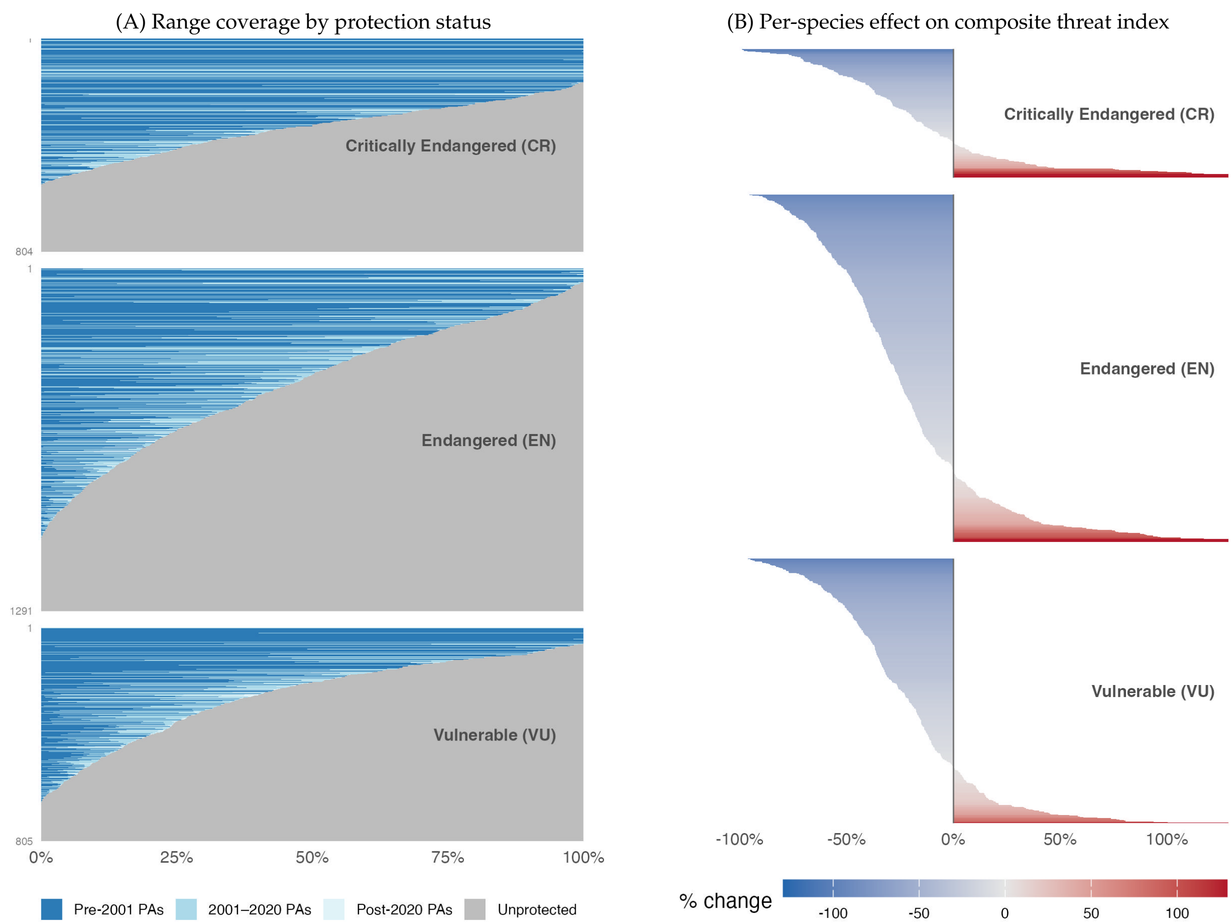

Figure C.10: **Species-level PA coverage and range-based effects — Amphibians.** Same as Figure C.9 but for threatened amphibians.

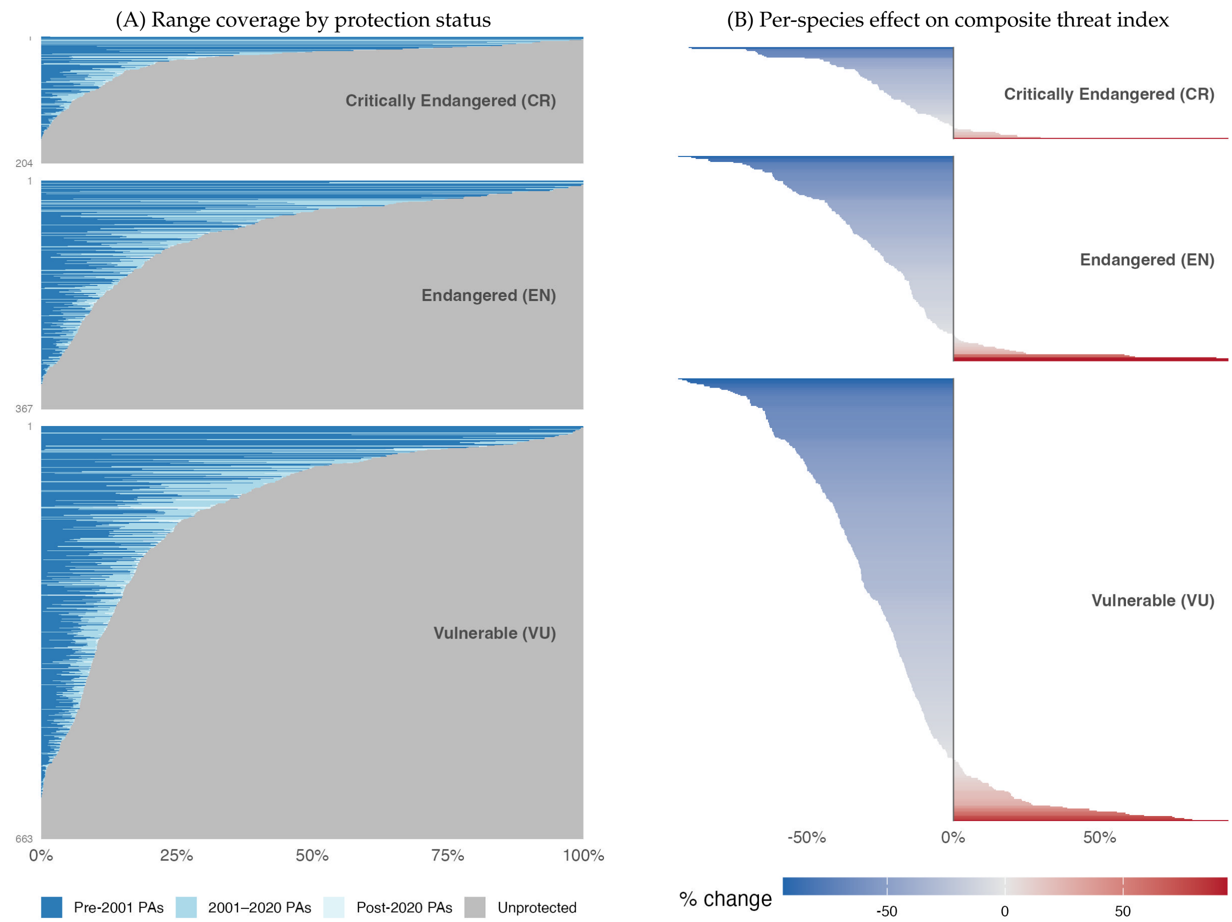

Figure C.11: **Species-level PA coverage and range-based effects — Birds.** Same as Figure C.9 but for threatened birds.

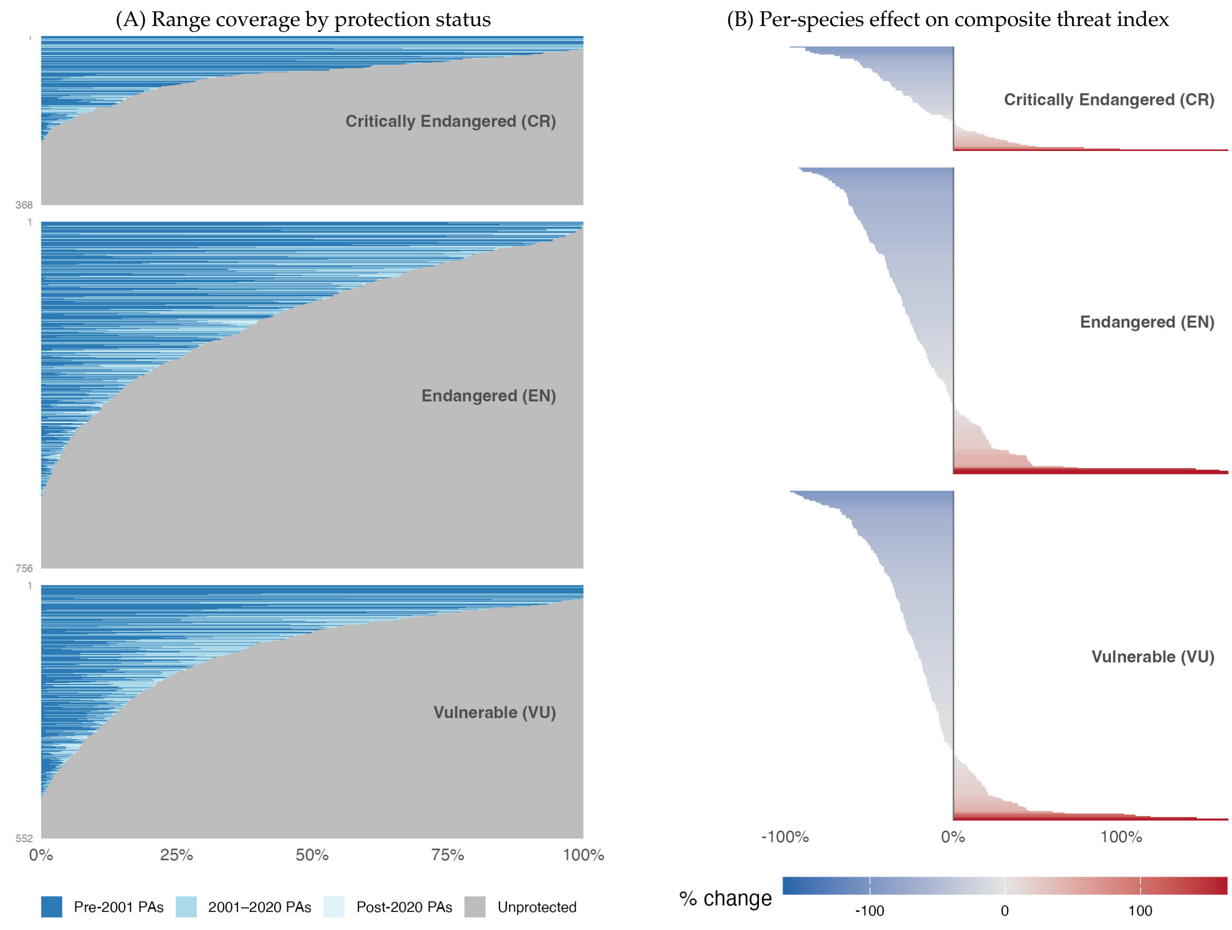

Figure C.12: **Species-level PA coverage and range-based effects — Reptiles.** Same as Figure C.9 but for threatened reptiles.

Supplementary Information References

1. Salafsky, N. *et al.* A standard lexicon for biodiversity conservation: Unified classifications of threats and actions. *Conservation Biology* **22**, 897–911 (2008).

2. Pesaresi, M. & Politis, P. GHS-BUILT-s r2023a - GHS built-up surface grid, derived from sentinel2 composite and landsat, multitemporal (1975-2030) (2023). URL http://data.europa.eu/89h/9f06f36f-4b11-47ec-abb0-4f8b7b1d72ea.

3. Potapov, P. *et al.* Global maps of cropland extent and change show accelerated cropland expansion in the twenty-first century. *Nature Food* **3**, 19–28 (2022).

4. Du, Z. *et al.* A global map of planting years of plantations. *Scientific Data* **9**, 141 (2022).

5. Gilbert, M. *et al.* Global distribution data for cattle, buffaloes, horses, sheep, goats, pigs, chickens and ducks in 2010. *Scientific Data* **5**, 180227 (2018).

6. Monitor, G. E. Global oil and gas extraction tracker (2022). URL https://globalenergymonitor.org/projects/global-oil-gas-extraction-tracker/.

7. Tang, L. & Werner, T. T. Global mining footprint mapped from high-resolution satellite imagery. *Communications Earth & Environment* **4**, 1–12 (2023).

8. Observatory, G. E., Google, of Technology in Stockholm, K. R. I., Enipedia & Institute, W. R. Global power plant database (2019). URL http://resourcewatch.org/.

9. Monitor, G. E. Global wind power tracker (2023). URL https://globalenergymonitor.org/projects/global-wind-power-tracker/.

10. Meijer, J. R., Huijbregts, M. A. J., Schotten, K. C. G. J. & Schipper, A. M. Global patterns of current and future road infrastructure. *Environmental Research Letters* **13**, 064006 (2018).

11. Programme, W. F. Global railways (2019). URL https://data.amerigeoss.org/dataset/global-railways1.

12. Arderne, C., Zorn, C., Nicolas, C. & Koks, E. E. Predictive mapping of the global power system using open data. *Scientific Data* **7**, 19 (2020).

13. Hansen, M. C. *et al.* High-resolution global maps of 21st-century forest cover change. *Science* **342**, 850–853 (2013). URL https://www.science.org/doi/10.1126/science.1244693.

14. Giglio, L., Boschetti, L., Roy, D. P., Humber, M. L. & Justice, C. O. The collection 6 modis burned area mapping algorithm and product. *Remote Sensing of Environment* **217**, 72–85 (2018).

15. Pekel, J.-F., Cottam, A., Gorelick, N. & Belward, A. S. High-resolution mapping of global surface water and its long-term changes. *Nature* **540**, 418–422 (2016).

16. Mulligan, M., van Soesbergen, A. & Sáenz, L. Goodd, a global dataset of more than 38,000 georeferenced dams. *Scientific Data* **7**, 31 (2020).

17. Li, X., Zhou, Y., Zhao, M. & Zhao, X. A harmonized global nighttime light dataset 1992–2018. *Scientific Data* **7**, 168 (2020). URL https://www.nature.com/articles/s41597-020-0510-y. Publisher: Nature Publishing Group.

18. Fischer, G. *et al.* Global agro-ecological zones v4 – model documentation. Tech. Rep., FAO, Rome (2021).

19. Zabel, F., Putzenlechner, B. & Mauser, W. Global agricultural land resources – a high resolution suitability evaluation and its perspectives until 2100 under climate change conditions. *PLOS ONE* **9**, e107522 (2014).

20. Pressey, R. L., Whish, G. L., Barrett, T. W. & Watts, M. E. Effectiveness of protected areas in north-eastern new south wales: recent trends in six measures. *Biological Conservation* **106**, 57–69 (2002).

21. Scott, J. M. *et al.* Nature reserves: Do they capture the full range of america's biological diversity? *Ecological Applications* **11**, 999–1007 (2001).

22. Venter, O. *et al.* Bias in protected-area location and its effects on long-term aspirations of biodiversity conventions. *Conservation Biology* **32**, 127–134 (2018).

23. Fick, S. & Hijmans, R. Worldclim 2: new 1km spatial resolution climate surfaces for global land areas. *International Journal of Climatology* **37**, 4302–4315 (2017).

24. Pearce-Higgins, J. W. *et al.* Geographical variation in species' population responses to changes in temperature and precipitation. *Proceedings of the Royal Society B: Biological Sciences* **282**, 20151561 (2015).

25. Gutiérrez-Hernández, O. & García, L. V. *Chapter 11 - Relationship between precipitation and species distribution*, 239–259 (Elsevier, 2021).

26. University, C. F. I. E. S. I. N.-C.-C. Documentation for the gridded population of the world, version 4 (gpwv4), revision 11 data sets (2018). URL https://sedac.ciesin.columbia.edu/data/collection/gpw-v4/documentation.

27. McKee, J., Chambers, E. & Guseman, J. Human population density and growth validated as extinction threats to mammal and bird species. *Human Ecology* **41**, 773–778 (2013).

28. Nelson, A. Estimated travel time to the nearest city of 50,000 or more people in year 2000 (2008). URL https://forobs.jrc.ec.europa.eu/products/gam/.

29. Schulze, K. *et al.* An assessment of threats to terrestrial protected areas. *Conservation Letters* **11**, e12435 (2018).

30. Joppa, L. N. & Pfaff, A. High and far: Biases in the location of protected areas. *PLOS ONE* **4**, e8273 (2009). URL https://journals.plos.org/plosone/article?id=10.1371/journal.pone.0008273. Publisher: Public Library of Science.

31. Olson, D. M. *et al.* Terrestrial ecoregions of the world: A new map of life on earth. *BioScience* **51**, 933 (2001). URL https://academic.oup.com/bioscience/article/51/11/933-938/227116.

32. Loucks, C., Ricketts, T. H., Naidoo, R., Lamoreux, J. & Hoekstra, J. Explaining the global pattern of protected area coverage: relative importance of vertebrate biodiversity, human activities and agricultural suitability. *Journal of Biogeography* **35**, 1337–1348 (2008).

33. Geldmann, J., Manica, A., Burgess, N. D., Coad, L. & Balmford, A. A global-level assessment of the effectiveness of protected areas at resisting anthropogenic pressures. *Proceedings of the National Academy of Sciences* **116**, 23209–23215 (2019). URL https://pnas.org/doi/full/10.1073/pnas.1908221116.

34. Gesch, D. B., Verdin, K. L. & Greenlee, S. K. New land surface digital elevation model covers the earth. *Eos, Transactions American Geophysical Union* **80**, 69–70 (1999).

35. UNEP-WCMC & IUCN. Protected planet: The world database on protected areas (WDPA) (2026). URL www.protectedplanet.net.

36. UNEP-WCMC. User manual for the world database on protected areas and world database on other effective area-based conservation measures: 1.6. Tech. Rep., UNEP-WCMC (2019). URL http://wcmc.io/WDPA_Manual.

37. Baylis, K. *et al.* Mainstreaming impact evaluation in nature conservation. *Conservation Letters* **9**, 58–64 (2016).

38. IUCN. The iucn red list of threatened species (2025). URL https://www.iucnredlist.org/en.

39. BirdLife International & Handbook of the Birds of the World. Bird species distribution maps of the world. version 2025.2. http://datazone.birdlife.org/species/requestdis (2025). Accessed on 25 February 2026.

40. IUCN. Species richness (spatial data). The IUCN Red List of Threatened Species. Version 2025-2. https://www.iucnredlist.org/resources/other-spatial-downloads (2025). Accessed on [DATE].